

Seismogenic Sources In The Adriatic Domain

Authors: Vanja Kastelic*, Paola Vannoli, Pierfrancesco Burrato, Umberto Fracassi, Mara Monica Tiberti, Gianluca Valensise

Istituto Nazionale di Geofisica e Vulcanologia – INGV, Via di Vigna Murata 605, 00143 Rome, Italy
* now at Istituto Nazionale di Geofisica e Vulcanologia – INGV, Via Arcivescovado 8, 67100 L'Aquila, Italy

Corresponding Author: Dr. Vanja Kastelic
Email address: vanja.kastelic@ingv.it
Phone: +39 08 62709110
Fax: +39 08 62709109

ABSTRACT

We present an overview of the seismogenic source model of the Adriatic domain included in the latest version of the DISS database (<http://diss.rm.ingv.it/diss/>) and in the European SHARE database (<http://diss.rm.ingv.it/SHARE/>). The model consists of Composite and Individual Seismogenic Sources located inside and along the margins of the Adria plate. In order to locate and parameterize the sources, we integrated a wide set of geological, geophysical, seismological and geodynamic data, either available from published literature or resulting from our own field work, seismic profile interpretations and numerical modelling studies. We grouped the sources into five regions based on geometrical and kinematic homogeneity criteria. Seismogenic sources of the Central Western Adriatic, North-Eastern Adriatic, Eastern Adriatic and Central Adriatic regions belong to the Northern Apennines, External Dinarides and offshore domains, respectively. They are characterized by NWeSE strike, reverse to oblique kinematics and shallow crustal seismogenic depth. Seismogenic sources of the Southern Western Adriatic region instead are EeW striking, dextral strike-slip faults, cutting both the upper and lower crust. The fastest moving seismogenic sources are the most southern thrusts of the Eastern Adriatic and the strike-slip sources of the Southern Western Adriatic, while the seismogenic sources of the Central Adriatic exhibit the lowest slip rates. Estimates of maximum magnitude are generally in good agreement with the historical and instrumental earthquake records, except for the North-Eastern Adriatic region, where seismogenic sources exhibit a potential for large earthquakes even though no strong events have been reported or registered. All sources included in the database are fully geometrically and kinematically parameterized and can be incorporated in seismic hazard calculations and earthquake or tsunami scenario simulations.

Keywords: Active tectonics, Seismogenic sources, Apennines, External Dinarides, Adriatic Sea

1. INTRODUCTION

The Adriatic Sea has long been considered a relatively undeformed crustal block and foreland area of the Apennines and External Dinarides thrust belts (e.g. Channell et al., 1979; Anderson and Jackson, 1987). Most of the largest earthquakes are distributed along the coasts and inland, while the seismic record for the offshore is less complete. Available geological data from standard active fault mapping cover the inland and coastal portions of some of the islands, but almost no data were reported for most of the offshore until recently (Grandić et al., 2007; Fantoni and Franciosi 2010). As new seismic profiles and borehole data were made available by hydrocarbon exploration, the attention shifted also towards the offshore areas. Such new data revealed a complex structural setting including inherited and reactivated normal faults, horst and graben geometries, NW-SE trending anticlines and evaporite bodies and active thrusts deforming Plio-Quaternary units. Moderate size earthquake sequences of the past few decades confirm the seismogenic activity of the faults in the Adriatic domain and at the same time call for a re-evaluation of the seismic potential in the entire region.

The outer thrusts of the Apennines and External Dinarides propagated into the Adriatic from the coastal areas towards the offshore, resulting in complex pattern of NW-SE trending anticlines, thrust faults and backthrusts and involving Late Pleistocene deposits. The two thrust fronts currently confront each other (Scrocca, 2006; Ivančić et al., 2006), a configuration that is somehow reminiscent of the proximity of Southern Alpine and Apennines fronts in the subsurface of the central Po Plain. In the southern Adriatic, morpho-bathymetry and seismic analyses (Ridente et al., 2008a; Di Bucci et al., 2009; Fracassi et al., 2012) revealed the presence of at least one major E-W, dextral, strike-slip fault stretching from the Gargano Promontory into the offshore. The southern eastern Adriatic is undergoing shortening and thrusting, but the external thrusts are less advanced than in the central Adriatic and generally follow the coastline.

Seismicity in the Adriatic domain is distributed both along the Adria plate margin and its interior (Renner and Slejko, 1994; Herak et al., 2005; Ivančić et al., 2006; Rovida et al., 2011) and shows prevailing compressional focal mechanisms (Renner and Slejko, 1994; Herak et al., 1995; Pondrelli et al., 2006; Pondrelli et al., 2011). The strongest earthquakes of the Adriatic domain occurred in the coastlines of the southern part of the Adriatic domain, while $M \geq 5.5$ earthquakes are typical for the entire region (Shebalin et al., 1974; Herak et al., 1995; Markušić et al., 1998; Herak et al., 2005; Papazachos et al., 2009; Thessaloniki Macroseismic earthquake catalogue, 2010; Rovida et al., 2011).

We aimed at building a seismogenic model of the Adriatic domain that could both improve the current understanding of the active tectonics and help assessing the local seismogenic potential. Our study was designed to integrate available data and recent advancements on the structural and seismological characteristics of the Adriatic domain into a homogenized and possibly uniform seismogenic source model. The Adriatic domain is not an easy area to characterize from the active tectonics point of view because most of the relevant geological and structural features are concealed by a thick recent sedimentary cover and by the sea. As a consequence, parameterization of the seismogenic sources is mostly based on geophysical subsurface data, covering only a small portion of the domain and often presenting contrasting interpretations. The fact that the Adriatic domain is shared among different countries inevitably implies a diverse level of geologic exploration and data availability. The model presented here attempts to overcome these limitations by 1) integrating all available data, 2) building on similarities between adjacent areas and 3) following common criteria for source characterization.

Our seismogenic source model consists of 38 Composite (CSS) and 23 Individual Seismogenic Sources (ISS) located inside and along the margins of the Adriatic domain, all of them structurally belonging to the external areas of the Central and Northern Apennines, the eastern Southern Alps, and the External Dinarides thrust belts. The geometrical and kinematical definition of each source is the outcome of integrated geological, geophysical, seismological, and geodynamic studies. These sources are included in the most recent version of the DISS database (<http://diss.rm.ingv.it/diss/>), a regional compilation originally covering the Italian territory (Valensise and Pantosti, 2001; Basili et al., 2008), and in the European SHARE database (<http://www.share-eu.org/>), an extension of DISS to the Euro-Mediterranean regions (Basili et al., 2010). The reader may refer to Basili et al. (2009) for a more detailed description on how the seismogenic source model was built. The fully parameterized seismogenic sources may serve as input data for various geodynamic and seismological applications, including regional probabilistic seismic hazard assessment (e.g. Meletti et al., 2008), large-scale geodynamic modelling (e.g. Barba et al., 2008; Cuffaro et al., 2010), studies on earthquake probabilities (e.g. Akinici et al., 2009, 2010), tsunami scenarios (e.g. Lorito et al., 2008; Tiberti et al., 2008), and strong-motion prediction models (e.g. Calderoni et al., 2012; Zonno et al., 2012).

2. GEOLOGICAL FRAMEWORK

The Adriatic Sea is a semi-closed basin of Meso-Cenozoic continental origin (e.g. Suess, 1883; Canavari, 1885; for a review see also Piccardi et al., 2011) surrounded by the Apennines and External Dinarides – Albanides thrust belts, having opposing vergence and defining its western and eastern margins, respectively, and by the S-verging Southern Alps to the north. Based on seismicity distribution and GPS measurements, the Adriatic domain has been interpreted either as a single microplate (Anderson, 1987; McKenzie, 1972), as the combination of two microplates joined along the Mid-Adriatic Ridge (e.g. Oldow et al., 2002; Scisciani and Calamita, 2009), or as two microplates connected roughly along the Gargano promontory-Dubrovnik alignment (e.g. Westaway, 1990; D'Agostino et al., 2008). Within this complex structural setting, the main factors causing and controlling the evolution of the circum-Adriatic region are 1) the subduction of the Adria plate below the Apennines and its east directed slab rollback (Doglioni et al., 1999; Wortel and Spakman, 2000); 2) the south-dipping slab of the European plate below the Southern Alps (Lippitsch et al., 2003); 3) the east-directed Adriatic slab under the External Dinarides (Piromallo and Morelli, 2003); 4) N to NE directed indentation of Adria into the Southern Alps and the External Dinarides. A high velocity crustal body connected to the indentation of Adria is recognized by various investigators beneath the Southern Alps and External Dinarides. structural units (Brückl et al., 2007; Šumanovac et al., 2009). A common characteristic of all bounding thrust belts is their orogenic transport towards Adria (e.g. Dewey et al., 1973; Dercourt et al., 1986). The Adriatic domain shows a northeast- to north-directed motion with respect to Eurasia (Babbucci et al., 2004; Battaglia et al., 2004; Grenerczy et al., 2005; D'Agostino et al., 2008; Devoti et al., 2008) and a higher lithospheric strength compared to its surroundings (Tesauro et al., 2009; Carafa and Barba, 2011). Geophysical and seismological investigation within Adria itself revealed the differences in the lithosphere structure between the northern and southern parts (Venisti et al., 2004).

The Eastern Southern Alps are the eastern portion of the late Cretaceous-Quaternary S-verging back-thrust belt of the Alpine chain, bounded to the north by the Insubric-Periadriatic line (Doglioni and Bosellini, 1987; Castellarin and Cantelli, 2000). The outer thrust front is composed by NE-SW to E-W trending faults and folds emerging along the mountain front or buried below the Quaternary foredeep and continental sediments of the Veneto-Friuli plain (Galadini et al., 2005), which were used to define the Neogene-Quaternary timing of activity of these structures (Caputo et al., 2010). To the east the Southalpine thrusts interact with the NW-SE trending, dextral strike-slip faults of the

Idrija fault system in the Slovenia border region (Bajc et al., 2001; Burrato et al., 2008; Kastelic et al., 2008).

The convergence along the eastern Adria margin since Late Jurassic first resulted in the formation of the Internal Dinarides (Tari, 2002). Thrusting gradually propagated westwards, as recorded by the migration of foredeep basin sequences in Late Cretaceous – Early Paleogene (Tari, 2002; Korbar, 2009), forming the External Dinaric thrust belt. The oldest thrusting activity associated with the External Dinarides in western Slovenia was recorded by Early Eocene foredeep flysch deposits (Drobne and Pavlovec, 1991). The onset of thrusting and related foredeep flysch deposition becomes younger southeastwards along the External Dinaric belt, and westwards in the offshore direction (Tari, 2002). Through Oligocene-Miocene times the foredeep basins progressively occupied the Adriatic offshore (Tari-Kovačić, 1998; Tari-Kovačić et al., 1998). Active faults in the External Dinarides are mostly NW-SE oriented, NE-dipping thrusts (Ivančić et al., 2006).

The outermost front of the NE-dipping External Dinarides lies adjacent to the SW dipping Northern Apennines outermost thrust front (Scrocca, 2006) in the middle of the Adriatic Sea. Different terms are used in the literature to refer to this region: Middle Adriatic Ridge (e.g. Finetti, 1982; Scisciani and Calamita, 2009), Adriatic Ridge (e.g. Scrocca, 2006) for its more central-western part, Central Adriatic Deformation Belt (e.g. Argnani and Gamberi, 1995), and Mid Adriatic Basin (e.g. Fantoni and Franciosi, 2010). The region is characterized by reactivated Permian-Triassic normal faults (Boccaletti et al., 2005; Scisciani and Calamita, 2009) that were inverted during the earlier compressional phases and subsequently cut by the Plio-Quaternary low-dipping thrust faults detaching at shallower levels (Scrocca et al., 2007). Such setting is confirmed by recent studies integrating seismic profiles (Grandić and Markulin, 2000; Fantoni and Franciosi, 2010) and earthquake data (Herak et al., 2005). The length of the Middle Adriatic Ridge is closely related to the occurrence of halokinetic structures (Geletti et al., 2008; Del Ben et al., 2010) that deform the youngest Pliocene-Quaternary syn-tectonic sediments (Grandić et al., 1999; Finetti and Del Ben, 2005; Herak et al., 2005; Geletti et al., 2008).

The Apennines thrust and fold belt developed in Neogene and Quaternary times in the hangingwall of a west-directed subduction zone (Carminati et al., 2004 and references therein) and is characterized by an inner extensional domain concentrated along the hinge of the mountain chain, and an external compressional domain along the Adriatic margin (e.g. Barchi, 2010 and references therein). Both domains migrated towards the northeast over time as a response to the progressive Adriatic lithosphere roll-back (e.g. Malinverno and Ryan, 1986; Royden et al., 1987; Doglioni et al., 1999; Faccenna et al., 2003). Compression is still active in the most external region along the NW-SE trending, low-angle faults (Scrocca, 2006).

The southern part of the Western Adriatic is characterized by the presence of the Apulia carbonate platform, a thick Meso-Cenozoic carbonate sequence overlying the Adriatic basement that crops out in the Gargano promontory, a ca. 50 km long, E-W trending relic of a contractional belt inherited from earlier deformation stages (Channell et al., 1979; Anderson, 1987; Bertotti et al., 1999; Catalano et al., 2001; Wortmann et al., 2001 and references therein). This area is dissected by a regional system of E-W trending, long-lived shear zones affecting the deeper portion of the crust roughly between 10 and 30 km depth (Morelli, 2002 and references therein). This deep-seated system lies within the current stress field caused by the NNW-SSE Africa-Eurasia convergence (e.g. Hippolyte et al., 1994) and is thought to have been reactivated in an oblique-right lateral sense, thus providing an explanation for the arcuate geometry of the southern Apennines thrust-belt and the Calabrian Arc up to eastern Sicily (Di Bucci et al., 2010). Some of these strike-slip faults are thought to be responsible for a number of strong earthquakes that struck the Gargano area and its

western surroundings both in historical and instrumental times (Fracassi and Valensise, 2007; DISS Working Group, 2010).

The distribution of historical (Gruppo di lavoro CPTI, 2004; Rovida et al., 2011) and instrumental earthquakes (Chiarabba et al., 2005; ANSS Catalog) (Figure 1) shows activity all along the Adriatic margin and inside the plate itself. Larger earthquakes take place in the southern parts of the Adriatic domain, while its central and northern portions are characterized by medium-sized events. Some of the studies argue that compressional deformation along the eastern Adriatic domain triggers predominantly extensional seismic activity along the Apennines due to strain induced by post-seismic relaxation (Mantovani et al., 1991; Viti et al., 2007).

GPS data show a general motion pattern toward the northeast and a magnitude decrease from the Adriatic towards the stable Eurasia (Grenerczy et al., 2005; Caporali et al., 2009; Devoti et al., 2008, 2011). Similar patterns are obtained also by finite element modelling of long-term strains in the eastern Adriatic and External Dinarides (Kastelic and Carafa, 2012).

3. INSIDE A SEISMOGENIC SOURCE

In our definition a Seismogenic Source is an active fault capable of releasing the accumulated stress through earthquakes. In this paper we present sources belonging to the DISS v. 3.2.0 database (<http://diss.rm.ingv.it/diss/>: DISS Working Group, 2010), covering the Italian territory and neighboring areas, further developed in the framework of the European Project SHARE (<http://diss.rm.ingv.it/SHARE/>) to cover the Euro-Mediterranean region. In the database we included only faults that can generate $M_w > 5.5$ earthquakes since this is the commonly accepted magnitude threshold above which a fault may leave a sizable signature in the geology and in the landscape.

The DISS database is a georeferenced web and stand-alone repository where seismogenic sources are presented in graphical as well as tabular form. Each source is completely parameterized with its 3D location and geometry, its kinematics and activity. For each given parameter, a qualifier and a note provide details on its characteristics and original data.

The location and geometry of the seismogenic sources described in this section follows a careful revision of geological, geomorphic and geophysical data combined with historical and instrumental seismicity data. The use of different datasets is useful to define and characterize in better detail the 3D structure of each seismogenic source.

We introduce seismogenic sources for active faults that 1) whose earthquake potential is documented by an instrumental, historical or paleoseismological record; 2) belong to a fault system where at least one of the faults possesses an instrumental, historical or paleoseismological earthquake record; or 3) are not associated with a particular earthquake, but given their geometry they can be activated within the current stress regime and show geomorphic evidence of their activity. In a process of introducing sources, we rely on published data but also on our own research based upon field-work, geomorphic analyses, analyses of earthquake and geophysical data.

In the following sections we briefly describe the two main categories of Seismogenic Sources that form the body of the database and show how their characteristics were constrained. A complete and detailed description of both source types can be found in Basili et al., (2008), Basili et al., (2009) and in the “Tutorial” section of the DISS web site (<http://diss.rm.ingv.it/diss/UserManual.html>).

3.1. COMPOSITE SEISMOGENIC SOURCES (CSSs)

A “Composite Seismogenic Source” (CSS) is constrained by geological and geophysical data and is characterized by geometric (strike, dip, width, depth) and kinematic (rake) parameters, but its length is loosely defined and spans an unspecified number of Individual Seismogenic Sources (ISSs, see paragraph 3.2). CSSs are based on regional surface and subsurface geological data and supported by additional seismological, geodynamic and geomorphic data that help constrain its parameters. They can host different magnitude earthquakes and their seismic potential can be derived from existing earthquake catalogues, geodynamic considerations and the characteristic seismogenic depth.

Contrary to ISSs, this category of sources was conceived to achieve completeness of the record of potential earthquake sources, although this may imply a smaller accuracy in their description. In conjunction with seismicity and modern strain data, CSSs can thus contribute to the development of regional probabilistic seismic hazard assessment and be used for investigating large-scale geodynamic processes (e.g. Barba et al., 2008; Meletti et al., 2008).

From a structural point of view, a CSS represents the leading fault plane of an active fault system, and is the potential source of the largest earthquakes. Based on this approach, we do not include in the database secondary structures or minor fault splays, as they are considered to be incorporated into the CSS. This general rule is not valid for splays or secondary structures that are large enough to host $M_w \geq 5.5$ earthquakes.

Each CSS is graphically shown as a polygon representing the surface projection of the seismically active fault plane, mapped with a given depth interval and average strike and dip angles. The position of the upper edge is highlighted with a polyline. The description of a CSS can be augmented by the description of associated fault scarps or fold axis data when available (usually structural features with documented Late Pleistocene – Holocene activity).

We have devised several possible ways to assign each CSS a maximum expected magnitude (M_{max}) (see also Table 2 in Basili et al., 2008, and Vannoli et al., in press): 1) the M_{max} associated with the largest ISS hosted in the CSS; 2) an M value obtained from a historical or instrumental catalogue for the larger earthquake associated with the given CSS, or for the larger earthquake of the surrounding region; 3) a value assigned using scaling relationships between M and source size (i.e. source width; notice that according with the definition for the CSS length, this parameter is not preferably used to infer M_{max}); 4) a value inferred from a physical model that includes deformation data of any sort (e.g. geodetic, seismic); or 5) a default $M=5.5$ when no other constraints are available.

Slip rate is the parameter that is most affected by the inhomogeneities among all the parameters we introduced, due to 1) differences in data availability, and 2) the time span these values refer to. When available, we relied on geological estimates for slip rates. Due to lack of more detailed studies for particular faults and due to the fact that many CSSs in the Adriatic domain lie offshore, we set the slip rate based on calculations from a finite element geodynamic modelling (Kastelic and Carafa, 2012) coupled with regional geological and geodetic data.

To illustrate how we operated in constructing the seismogenic source model for the Adriatic domain, in the following paragraph we describe in some detail the process of identification and parameterization of a Composite Seismogenic Source. All our Composite Sources were derived using the same standards as in the example presented.

3.1.1. HRCS020 - Eastern Adriatic offshore – Central

The HRCS020 CSS is located in the Central Adriatic that is characterized by the presence of two thrust belts with opposite vergence – the Apennines to the west and the External Dinarides to the east. The geological and structural conditions of this area differ from those of the western and eastern Adria margin and further inland. In the literature this area is often referred to as Mid Adriatic Ridge (e.g. Finetti, 1982; Scisciani and Calamita, 2009), Adriatic Ridge for its central-western part (e.g. Scrocca, 2006), Central Adriatic Deformation Belt (e.g. Argnani and Gamberi, 1995) or Mid Adriatic Basin (e.g. Fantoni and Franciosi, 2010). It is characterized by NW-SE structural highs (Grandić and Markulin, 2000; Scrocca et al., 2007) related to thrust-related folding (Argnani and Frugoni, 1997), active diapirism (Geletti et al., 2008; Del Ben et al., 2010) or to a combination of both processes (Bally et al., 1986). The Cenozoic compressional tectonic setting in this area was preceded by the Mesozoic extension and its horst-graben structural setting. Seismic and borehole data show that the early stages of compression caused the inversion of older normal faults (Scrocca et al., 2007; Scisciani and Calamita, 2009), while in the Plio-Quaternary the active thrusting was superimposed on the basement-involving normal faults (Scrocca et al., 2007) and shows lower dip angles with respect to older normal faults (Scrocca et al., 2007; Fantoni and Franciosi, 2010). Earthquake activity confirms that active compression is accommodated by thrust planes (Herak et al., 2005) showing gentler dips with respect to the normal faults.

The HRCS020 Source is located in the central part of the Central Adriatic. The sea-bottom of the area is covered by a layer of Quaternary and Pleistocene fluvial deposits underlain by Neogene (predominantly Pliocene) foredeep sedimentary clastics that overlie the earlier stage Eocene to Miocene foredeep flysch deposits (Fantoni and Franciosi, 2010). Deeper stratigraphic units consist of Mesozoic platform carbonates, Permian and Triassic clastic rocks with evaporite layers and Variscan basement units (Grandić and Markulin, 2000; Fantoni and Franciosi, 2010). An evaporite diapir rising from the Permian and Triassic host rocks towards the surface and protruding all the way to the sea-bottom is known to occur in this area (Grandić and Markulin, 2000; Geletti et al., 2008). The Jabuka shoal is formed by Triassic-Jurassic gabbro that appears to belong to the core of a small magmatic body (Juračić et al., 2004). The presence of magmatic rocks on the sea floor aligned in a narrow patch of NW-SE to WNW-ESE direction is attributed to thrust activity (Juračić et al., 2004; Herak et al., 2005), or to uplift processes connected to diapirism uprise (Grandić et al., 1999). The latter option is supported by the presence of both magmatic rocks and evaporites on the Jabuka island (Geletti et al., 2008).

The HRCS020 Source (Figure 5) represents an active thrust fault uplifting the gabbro body in its hangingwall across the evaporites lying in the footwall of the fault (Herak et al., 2005). To establish its location and parameters, we relied on seismic profiles (Grandić and Markulin, 2000; Grandić et al., 2002; Fantoni and Franciosi, 2010), gravity (Grandić et al., 2002), borehole (Grandić et al., 2002) and earthquake data (Herak et al., 2005). The HRCS020 Source originates in the Variscan basin and cuts through the Permian and Triassic clastic rocks, Mesozoic carbonates and Paleogene and Neogene foredeep rocks. The depth of the upper edge of the source, that is the minimum depth to which the dynamic earthquake rupture propagates based on the local geological characteristics of the fault area, is set to 2 km below sea level. The maximum source depth is set at 12 km based on seismic profiles (e.g. Fantoni and Franciosi, 2010) and earthquake data (Herak et al., 2005). The strike of the fault was determined in the 270°-300° range based on the map of active faults of the area (Ivančić et al., 2006) and on the focal mechanisms of the 29 March 2003, Mw 5.5 Jabuka earthquake (Herak et al., 2005; Global CMT Catalog, available at <http://www.globalcmt.org/>) that occurred on a segment of the HRCS020. The dip was set in the range 35°-60° based on seismic profiles (e.g. Fantoni and Franciosi, 2010) and focal mechanism data (Herak et al., 2005), while the rake was set in the range 70°-100° mainly based on earthquake and regional geological data. Based upon the results of geodynamic numerical modelling (Kastelic and Carafa, 2012) compared with

geologically estimated values, we set the slip rate for this source to be between 0.05 and 0.20 mm/yr. Based upon the geometrical characteristics of the fault and the available data on neighbouring faults and regional data, we estimate a M_{max} equal to 6.0.

The geometry of the HRCS020 was modified with respect to the previous versions of DISS, where it was part of a longer Eastern Adriatic Offshore Source (HRCS004) that encompassed what currently are three separate CSSs (HRCS021, HRCS020 and HRCS004, from north to south). During the revision process based on new available geological and geophysical information, we divided the longer source to better capture the geometrical characteristics of different segments of the fault system. The solution presented here and adopted by the DISS v. 3.2.0 and SHARE databases better describes the along-strike geometric (i.e. strike and dip) and activity (i.e. slip rate, as supplied by Kastelic and Carafa, 2012) characteristics. By presenting three seismogenic sources instead of a longer one, we do not imply any change in the seismogenic potential of this part of our model. Nevertheless, capturing the complexity of the sources in greater detail may return more accurate estimates of the expected ground shaking and tsunami potential to be used in Seismic Hazard Assessments (SHA).

3.2. INDIVIDUAL SEISMOGENIC SOURCES (ISSs)

An “Individual Seismogenic Source” (ISS) is obtained from geological and geophysical data and is characterized by a full set of geometric (strike, dip, length, width and depth), kinematic (rake) and seismological parameters (average displacement, magnitude, slip rate, recurrence interval). ISSs are assumed to exhibit “characteristic” behavior with respect to rupture length/width and expected magnitude. They are tested against worldwide databases for internal consistence in terms of length, width, average displacement and magnitude, and can be complemented with information on active fault scarps and fold axis when present (structural features with documented Late Pleistocene – Holocene activity). This category of sources is intended to supply the most accurate information available for the best identified faults, but the completeness of the sources dataset cannot be guaranteed. As such, they can be used for calculating the probability of the occurrence of strong earthquakes generated by any individual source (Akinci et al., 2009, 2010), for calculating earthquake and tsunami scenarios (Lorito et al., 2008; Tiberti et al., 2008), and for tectonic and geodynamic investigations, but they are not meant to comprise a complete input dataset for SHA.

An ISS is a segment, section or part of a CSS (i.e. is a fault segment of a fault system), responsible for a specific $M \geq 5.5$ historical or instrumental earthquake. A CSS may host a single or multiple ISSs, depending on data available for the detailed study necessary to identify an ISS. If the geological and geophysical data available for a specific $M \geq 5.5$ earthquake are not detailed enough to grant the compilation of the responsible ISS, the earthquake will be “accounted for” only by its parent CSS. In certain cases (e.g. ITIS031 and ITIS032; Figure 7) an ISS may not be associated with a known historical or instrumental earthquake, but its existence may be based on geological and structural evidence detailed enough to constrain its geometry and to document its recent activity. Such ISS effectively represents a potential seismic gap. A case of such ISS type can be an individual blind thrust producing an antiform of certain geometry and dimensions to allow for a parametrization of the blind thrust geometry and based on those the parameters for the correspondent ISS. In order for such blind thrust to be considered active and thus seismogenic and a potential seismogenic source, it needs to exhibit certain markers of its recent activity like displaced recent sediments or it needs to effect the local fluvial pattern due to its growth.

Similarly to what we did for the CSSs, in the following section we describe how we constrained the parameters of an Individual Seismogenic Source of the Adriatic domain. All our Individual Sources were derived by the same procedure.

3.2.1. HRIS001 - Jabuka Island

The HRIS001 Jabuka Island Individual Source is a portion of the Eastern Adriatic offshore – Central CSS that is thought to be responsible for the 29 March 2003, Mw 5.5 earthquake. Its location, geometry and maximum earthquake potential were obtained mainly from the work by Herak et al. (2005), coupled with focal mechanism solutions from various catalogues (e.g. Global CMT Catalog and Pondrelli et al., 2006, European-Mediterranean RCMT Catalog, available at <http://www.bo.ingv.it/RCMT/>). The magnitude of the earthquake was used to scale the length and width of the HRIS001 Source through the Wells and Coppersmith (1994) empirical relationships; the uniform coseismic slip was assessed through the Hanks and Kanamori (1979) analytical relationships. Based on these assumptions we conclude that the 2003 earthquake was caused by 0.24 m of slip over a 5.3 km-long and 4.9 km-wide plane. The minimum and maximum depths of the source are 3.0 and 6.3 km, respectively. Based on the available focal solutions we assigned the source a 269° strike, 42° dip and 70° rake. The 0.05-0.20 mm/yr assigned slip rate is constrained by geodynamic modelling and geological considerations (Kastelic and Carafa, 2012) and can be extended also to the parent CSS. Assuming characteristic earthquake behavior and based on the the average displacement and slip rate, we calculated a recurrence interval in the range 1200 to 4800 years.

The P-axis estimated from the earthquake data (Global CMT and RCMT catalogs) is nearly horizontal and trends almost north-south. It is parallel to the orientation of regional compression based on geological measurements (Prelogović et al., 2003) and with the strain field obtained from GPS measurements (Oldow et al., 2002).

4. SEISMOGENIC MODEL

This section contains a description of all seismogenic sources of the Adriatic domain included in the version 3.2.0 of DISS (<http://diss.rm.ingv.it/diss/>). For this area the new release of DISS contains a substantially larger number of new sources than the previous versions, and we also updated the parameters of the already existing sources. Our seismogenic model of the Adriatic domain contains 38 CSSs and 23 ISSs. We subdivided the Adriatic region into five regions, based on their structural setting, faulting style, and location. The five regions terminate to the south at the latitude of the Mattinata-Gondola Fault System (Figure 1) and southern Montenegro. For each region we describe the geological and geophysical background derived from original and literature data that we collected or interpreted. Each region is identified by a name based on its location and by a code, formed by the acronym of the Adriatic Domain (AD) and a sequential number, assigned in a clockwise fashion moving around the Adriatic Sea starting from the north (Figure 1a). Therefore, the regions are described beginning from the North-Eastern Adriatic area; within each region, each CSS will be described from north to south and from west to east. The five regions are: North-Eastern Adriatic (AD1), Eastern Adriatic (AD2), Central Adriatic (AD3), Southern Western Adriatic (AD4), and Central Western Adriatic (AD5) (Figure 1a).

4.1. North-Eastern Adriatic – AD1

The seismogenic sources included in AD1 encompass the Gulf of Trieste and the inner Istria Peninsula at the northernmost end of the Adriatic Sea (Figure 3). These sources belong to the External Dinarides thrust system, which at this end is relatively less advanced than elsewhere in the Eastern Adriatic region (AD2, see section 4.2).

Faulting in this sector of the External Dinarides thrust system is characterized by reverse to reverse-dextral kinematics, as testified by fault plane solutions and by structural and geological kinematic indicators. This circumstance is confirmed by GPS velocity solutions, which locally show the N-S directed shortening (e.g. Devoti et al., 2011) that is ultimately responsible for the tectonic and seismic activity of the Friuli and Italian-Slovenian border region (e.g. Burrato et al., 2008; Kastelic et al., 2008). Horizontal maximum stress indicators (Heidback et al., 2010; Montone et al., 2012) show NNE to NE oriented vectors, consistent with strike-slip to thrust faulting regime on NW-SE oriented fault planes.

In contrast with the adjacent portions of the Southern Alps, with the area around the Idrija fault system and with the External Dinarides, seismicity in this region is very limited. Instrumental earthquakes of magnitude < 3.0 concentrate near the south-eastern portion of AD1 near the town of Rijeka. The strongest historical earthquake associated with one of the four composite seismogenic sources of AD1 is the 14 August 1574, Mw 5.6 Lupoglav earthquake, investigated in detail by Cvijanović (1981) and currently listed in the CPT111 Catalogue (Rovida et al., 2011).

Only one tsunami has been reported to have hit the coasts of this region in historical times; that is the event that flooded Venice and Trieste on 26 March 1511 (Pasarić et al., 2012). This tsunami is traditionally associated with the 26 March 1511, Mw 7.0 Idrija earthquake that struck the border region between Italy and Slovenia on the same day (Rovida et al., 2011). On the basis of geological evidence and of the distribution of the damage, however, the seismogenic source of this earthquake is considered to be the Idrija Fault (Burrato et al., 2008, Fitzko et al., 2005), a large NW-SE trending strike-slip fault belonging to the External Dinaric fault system located well inland in Slovenia that is thought to be responsible also for the of 12 April 1998, Mw 5.7 Bovec and 12 July 2004, Mw 5.2 Krn Mountains earthquakes (Bajc et al., 2001; Kastelic et al., 2008). These circumstances suggest a non-tectonic origin for the 1511 tsunami, like studied also by Camassi et al. (2011).

In spite of the lack of seismicity in AD1, we decided to include in our database four seismogenic sources whose recent activity is demonstrated by geophysical and geological evidence (Busetti et al., 2010). In doing so we stress the importance of including also slow moving active faults in the SHA of seismically silent areas (Slejko et al., 2011).

The four seismogenic sources included in this region represent the north-western continuation of the outer External Dinaric thrust front of the Croatian coastal area, included in DISS as the HRCS025 Krk source (described in 4.2).

The most external fault represents the overthrusting of Eocene Flysch over Mesozoic limestones. It has been mapped in Istria as the Buzet thrust fault (Placer et al., 2004; see also profile 1 in Figure 2), while in the Trieste Gulf it was imaged by the CROP M-18 deep seismic profile (Finetti and Del Ben, 2005; Scrocca et al., 2003), and more recently by high resolution shallow seismic investigations (Busetti et al., 2008; 2010). This thrust front includes the HRCS029 Lupoglav and the ITCS101 Southern Trieste Gulf sources. Conversely, the more internal structure is the main thrust of Mesozoic limestones over Eocene flysch, known as the Črni Kal thrust fault and Trieste fault zone (see also profile 1 in Figure 2). The former is known due to geological field mapping (Plenicar et al., 1969; Šikic et al., 1972), while the latter was investigated in detail by means of the same geophysical dataset used to highlight the structural configuration of the Trieste Gulf (Busetti et al., 2008, 2010). This thrust front includes the HRCS032 Trstenik, and the ITCS100 Northern Trieste Gulf sources.

The geometric and kinematic parameters of the four CSSs were constrained as follows (see also Figure 3). The minimum and maximum depth were inferred from regional geological and geophysical observations and earthquake data. The strike is based on geological and structural data that define the mean orientation of the thrust fronts; for the two Croatian sources it is based on geological mapping by Placer (2007), Pleničar et al. (1969) and Šikić et al. (1972). The two sources of the Trieste Gulf were described by Buseti et al. (2008; 2010). The dip of the four seismogenic sources was derived from regional structural and seismotectonic data, and from seismic profiles and seismotectonic considerations, where available (e.g. Buseti et al., 2008; Kuk et al., 2000). The rake was inferred from regional structural and earthquake data (focal mechanisms and horizontal maximum stress orientations combined with the geometry of the sources). The slip rate, ranging from 0.10 to 0.30 mm/yr for all the four sources, was inferred from finite element modeling and geodynamic considerations (Kastelic and Carafa, 2012). The maximum magnitude was inferred from fault geometry, associated historical and instrumental earthquakes and regional considerations; the strongest event is the 14 August 1574, Mw 5.6 Lupoglav earthquake, associated with the HRCS029 Source.

In AD1, the two sources located along the outer thrust (HRCS029 and ITCS101) are slightly shallower and more gently dipping than the two sources representing the inner thrust (HRCS032 and ITCS100), and are characterized by a smaller maximum magnitude.

Complete parameters for the CSSs and ISSs of AD1 are supplied in Figure 3.

4.2. Eastern Adriatic – AD2

AD2 includes the coastal, island and offshore areas of Croatia, Bosnia and Herzegovina, and Montenegro (Figure 4). It spans over 600 km along the NW-SE oriented Eastern Adriatic coast line and reaches across-belt width of about 100 km. AD2 contains 14 CSSs and three ISSs belonging to the central part of the External Dinarides thrust belt.

The structural style of the External Dinarides is dominated by rigid carbonate rocks, whose shortening started with ramping along deep decollements from the root zone, with a south-western tectonic transport direction in an in-sequence thrust propagation scheme (Tari, 2002). The prevailing structural elements of the External Dinarides are the NW-SE striking thrust/reverse faults and the associated anticlines.

GPS data for AD2 display a general NNE-SSW to NE-SW trend of horizontal motion, with velocities of 2.0 - 2.5 mm/yr in northern AD2 (Grenerczy et al., 2005) and up to 4.0 - 4.5 mm/yr in the central and southern External Dinarides (Bennett et al., 2008; Devoti et al., 2008; 2011; Grenerczy et al., 2005). This pattern is consistent with the results of geodynamic modelling (Kastelic and Carafa, 2012) and is in agreement with the orientation of the maximum compressional stress obtained from structural analysis and field surveys (Prelogović et al., 2003).

Both instrumental and historical data show earthquake activity across the entire width of the External Dinarides thrust belt. Unfortunately, the earthquake catalog available for AD2 is not homogeneous and completely lacks reliable estimates of macroseismic magnitudes in the central part of the region, for which only intensities estimates are provided (Shebalin et al., 1974). The strongest earthquake recorded in the AD2 is the 15 April 1979, Mw 7.1 Montenegro event (Benetatos and Kiratzi, 2006), which occurred in the southern part of AD2, where the strongest known earthquakes concentrate. Other important earthquakes of the same area are the 4 August 1608, Mw 6.3, Herzegovi, 28 July 1639, Mw 6.8, Dubrovnik, 6 April 1667, Mw 7.2, Montenegro, 1699, Mw 6.2, Ulcinj, and 11 January 1962, Mw 6.1 Makarska, (Herak et al., 1995; Papazachos et

al., 2009; Thessaloniki Macroseismic Database, 2010) ones. No strong events are reported in the northern portion of AD2, but a number of $M_w > 5.5$ events are known from historical catalogues, such as the 1323, M_w 6.0, Novi Vinodolski, 12 January 1721, M_w 6.1, Rijeka, and 1 March 1870, M_w 5.6, Gorski Kotar earthquakes (Rovida et al., 2011). Using macroseismic estimates, Shebalin et al. (1974) report an intensity IX event on 30 June 1343 and three intensity VIII events on 1648, 1844 and 1878.

Available focal mechanisms (Herak et al., 1995; Pondrelli et al., 2006) and structural geological data show that thrusting is the prevailing mode of deformation along the coast and in the islands, whereas more complex kinematics on steeper fault planes with reverse, strike-slip and oblique motion prevail in the inner parts of the belt.

Several tsunamis of seismic, landslide and meteorological origin have been reported for AD2 (Pasarić et al., 2012; Soloviev et al., 2000). Earthquake-generated tsunamis are more frequent in the southern part of the area (Figure 1b), where the two largest tsunamis were associated with the 6 April 1667 Dubrovnik and with the 15 April 1979, Montenegro earthquakes. A smaller tsunami was caused by the 11 January 1962 Makarska event.

In AD2 we identify 14 CSSs: HRCS001, HRCS002, HRCS005-HRCS008, HRCS012, HRCS013, HRCS015, HRCS016, HRCS018, HRCS025, MECS001, MECS007, and three ISSs: HRIS002, HRIS003, HRCS004 (see Figure 4 and the eastern end of the geological sections of Figure 2).

The prevailing strike of the CSSs in AD2 is NW-SE, except for HRCS002 and HRCS007 that are more E-W oriented (Figure 4). Strike was determined based on seismic reflection (Grandić et al., 2004) and structural and geologic data (Blašković, 1999; Ivančić et al., 2006; Grandić et al., 2007; Prelogović et al., 1998). A common characteristic of these sources is their NE to N dip, while the faults underlying the islands and the coast exhibit a gentler dip with respect to the more internal sources. The northwesternmost sources exhibit a steeper dip, while MECS001 and MECS007 are shallower dipping. Information on fault dip was based on seismic reflection data (Grandić et al., 2004) and on the seismotectonic characteristics of earthquake sequences (Benetatos and Kiratzi, 2006; Herak et al., 1995; Kuk et al., 2000). The prevailing kinematic style is thrusting to reverse. HRCS002 and HRCS007 exhibit a significant left-lateral component while HRCS005, HRCS006 and HRCS025 exhibit reverse-right lateral kinematics. The average rake value has been set based on structural data (Grandić et al., 2004), seismotectonic cross-sections (Kuk et al., 2000), and earthquake data (Herak et al., 1995).

All sources in AD2 are located in the upper crust with maximum depth of 18 km for HRCS005 and HRCS008, and are interpreted as deep-seated, basement involving thrusts (Grandić and Markulin, 2000; Grandić et al., 2004). Fantoni and Franciosi (2010) proposed an alternative interpretation of the fault geometry of a shallower dipping ramp connected to a flat at 8-10 km depth (see Section 2 in Figure 2). Our solution takes into account the occurrence of a continuous belt of seismicity reaching depths down to about 18 km as shown by Kuk et al. (2000).

The differences in the maximum depth of the seismogenic sources that may arise using the different interpretation of the seismic lines, result in large variations of the width and hence in the estimation of the maximum magnitude event (M_{max}).

M_{max} was assigned based on the local seismic catalogues and on the geometric characteristics of the sources. The largest values are assigned to HRCS001 and MECS001, which in the past hosted $M_w \geq 7$ earthquakes (in 1667 and 1979, respectively). The other sources were assigned a $M_{max} > 6$, except the HRCS007 and HRCS018 that were assigned a M_{max} 5.8.

Slip rates were set based on the results of geodynamic modeling (Kastelic and Carafa, 2012). The highest value is characteristic for the MECS001 Source and spans over the 0.9-2.0 mm/yr interval. The regional slip rate trend is the decrease towards the NW of AD2, to values of 0.1-0.4 mm/yr. For HRCS006 we also calculated the vertical submergence rate based upon the current elevation of a submerged notch with respect to a regional reference value (Benac et al., 2004; 2008; Kastelic et al., unpublished data) and used dislocation modeling based on fault plane geometry to obtain the fault slip rate.

Three ISSs are located in AD2, HRIS002, HRIS003 and HRIS004, corresponding to the 5 September 1996, Mw 6.1, Ston, 11 January 1962, Mw 6.1, Makarska and 7 January 1962, Mw 5.9, Makarska earthquakes, respectively. All sources were balanced based on the recorded magnitude, their geometry, size (length, width) and average slip through empirical (Wells and Coppersmith, 1994) and analytical (Hanks and Kanamori, 1979) relations to optimize their parameters. HRIS002, belonging to the HRCS001 Composite Source, is a low angle thrust plane placed between 5.8 and 10.5 km depth; it is 11.0 km-long and 8.8 km-wide and its estimated average slip-per-event is 0.4 meters, yielding a recurrence interval of 286-2000 years. Both the HRIS003 and HRIS004 ISSs belong to the HRCS002 and represent the patches of the CSS activated in two events of the 1962 seismic sequence. They are intermediate-dipping reverse faults with a component of left lateral slip. HRIS003 corresponds to the 1962 sequence mainshock; it is a 11.9 km-long, 8.8 km-wide fault located between 4.2 and 11.9 km depth and displaying an average slip-per-event of 0.58 meters, which combined with the full range of slip rate yields a recurrence interval of 414-1993 years. HRIS004 represents a part of the HRCS002 activated during a foreshock of the 1962 seismic sequence. Its dimensions reach 12.0 km in length and 7.1 km in width; it is located between 5.2 and 9.8 km depth and has an average slip-per-event of 0.37 meters. Its recurrence interval falls in the range 264-1233 years.

Complete parameters for the CSSs and ISSs of AD2 are supplied in Figure 4.

4.3. Central Adriatic – AD3

The Central Adriatic region (AD3) comprises the offshore areas of Italy and Croatia and is characterized by the compression due to thrust belt propagation of both the Apennines and the External Dinarides. It is a 400 km-long, 100 km-wide, roughly rectangular area extending in the NW-SE direction parallel to the both eastern and the western coast of the Adriatic Sea. AD3 hence includes six Composite (HRCS004, HRCS010, HRCS014 HRCS020, HRCS021 and ITCS052) and one Individual (HRIS001) Seismogenic Sources lying in the external parts of the External Dinarides and of the Apennines thrust belts (Figure 5). The structural setting of the Central Adriatic was described in the paragraph 3.1.1. Due to its offshore location, the historical earthquake record available for AD3 is very limited and no direct GPS measurements exist. Some historical earthquakes that have been located inland could in fact have occurred offshore, in which case also their magnitude estimate would be biased. In addition to that, small to medium size pre-instrumental earthquakes occurring offshore at a significant distance from a populated island or from the coast could have gone unreported. The advent of the instrumental era somehow bridged this issue, but the problem of precisely locating offshore earthquakes still remains due to the limited density of the available networks.

Only one earthquake above Mw 5.5 is reported by the CPTI11 seismic catalogue (Rovida et al., 2011) in AD3; the 7 February 1844, Mw 5.6 Basso Adriatico earthquake (Figure 5). A previous version of the same catalogue (Gruppo di lavoro CPTI04, 2004) reported also the 30 November 1934, Mw 5.8 earthquake at a location consistent with the position of HRCS021. The CPTI11

catalogue lowered the magnitude of this earthquake below the 5.5 level and located it more to the NE. This example outlines the difficulties of dealing with offshore areas. The instrumental seismicity records report a Mw 5.5 earthquake on 29 March 2003 (Herak et al., 2005) that is consistent with the HRCS020 CSS. Several earthquakes in the magnitude range 4.0 to 5.5 that can be associated with the CSSs of AD3 are reported for the Central Adriatic. A well investigated sequence associated with HRCS004 took place with a mainshock on 26 April 1988, Mw 5.4 (Gruppo di lavoro CPTI04, 2004; Markušić et al., 1990).

Available focal mechanism solutions (Pondrelli et al., 2006) show thrusting along NW-SE trending intermediate dipping fault planes to be the dominant style of the region. A N005°-N010°-trending horizontal velocity vector of 2-3 mm/yr was calculated for the region concordant to the AD3 using a finite element geodynamic modeling technique (Kastelic and Carafa, 2012). Such trend is consistent with the orientation of the maximum compressional stress obtained from structural data (Prelogović et al., 2003).

A common characteristic of the composite sources of AD3 is their NW-SE strike and their thrust kinematics on medium dipping fault planes. The ITCS052 Source has a SW dip direction and corresponds to an external low dip angle thrust of the Apennines thrust belt (Scrocca et al., 2006). On the contrary, the HRCS004, HRCS010, HRCS014 HRCS020, HRCS021 Sources have a NE directed dip and we assign them to external structures of the External Dinarides belt related to the westward propagation of compression along the eastern Adriatic margin. Such characteristics of AD3 Seismogenic Sources were set in accordance with seismic reflection data (Fantoni and Franciosi, 2010; Finetti and Del Ben, 2005; Grandić and Markulin, 2000; Scisciani and Calamita, 2009; Scrocca, 2006) and seismotectonic considerations (Herak et al., 2005). The seismogenic Sources belonging to the External Dinarides reach higher depths (12 km) with respect to the Apennines external source (8 km), and thus are thought to deform the entire stratigraphic sequence from the Variscan basement to the Neogene foredeep rocks (Figure 2). The seismic character of the maximum depth range is confirmed by earthquake presence at those depths (Herak et al., 2005). On the contrary ITCS052 is limited to the Mesozoic carbonate sequence. The difference in seismogenic depth among the sources is reflected also in their assigned Mmax. External Dinarides thrusts are thought to be capable of producing earthquakes up to Mw 6.0, while ITCS052 was assigned a Mmax 5.5. Mmax for the AD3 sources was assigned based on the seismic catalogues and on the geometric characteristics of the sources.

Slip rates for the External Dinarides Sources were set to 0.05 – 0.20 mm/yr based on the results of geodynamic modelling (Kastelic and Carafa, 2012), while the slip rate interval for the Apennines external source was estimated from geological data in the range 0.10 – 0.50 mm/yr.

The HRIS001 source is a part of the HRC020 Source activated during the 29 March 2003, Mw 5.5, Jabuka earthquake. The characteristics of the fault were set taking into account the scaling among the magnitude, geometry (length and width) and average fault slip through empirical (Wells and Coppersmith, 1994) and analytical relations (Hanks and Kanamori, 1979) respectively. A more detailed description of the Jabuka ISS is given in 4.2.1.

Complete parameters for the CSSs and ISSs of AD3 are supplied in Figure 5.

4.4 Southern Western Adriatic – AD4

The Southern Western Adriatic region (AD4) encompasses three main deep-seated (in the 10-30 km depth range) E-W trending shear zones that affect the Apulian foreland including portions of the Adriatic crust beneath the external Apennines thrust belt; the Northern Abruzzo shear zone, the Tremiti Line, and the Molise-Gondola shear zone (Figure 1b). Onshore, AD4 straddles a sector of coastal central Italy from northern Abruzzo to northern Puglia. AD4 also includes a sizable region

offshore the Gargano promontory and its marine surroundings. AD4 thus spans ca. 250 km from west to east and ca. 100 km from north to south.

AD4 includes three sub-parallel regional fault systems (Figure 6) broken down into six CSSs (Figure 6). Each CSS includes at least one ISS; as a whole, AD4 includes nine ISSs.

AD4 is a peculiar area in the complex tectonics of the Adriatic microplate domain. While the majority of Adria is encircled by intense deformation and seismicity along its collisional margins (Figure 1; Anderson, 1987; Anderson and Jackson, 1987; Channell et al., 1979; Favali et al., 1993; Finetti, 1984; Finetti et al. 1987; Lort, 1971; McKenzie, 1972), well accounted for by AD1-AD2, the tectonics of AD4 is strongly controlled by the inherited, regional, long-term structural segmentation that commonly affect foreland basins (Allen et al., 1986). As discussed in the literature (e.g. Doglioni et al., 1994), foreland deformation can evolve into complex strike-slip fault systems that accommodate large-scale strain partitioning during active subduction and continental collision. On an all-Adriatic domain scale, and within the present stress field following the geodynamic change postulated by Hippolyte et al. (1994), we hypothesize that a whole set of regional, deep-seated, ca. E-W trending fault systems has been reactivated in a right-lateral, oblique motion, due to NNW-SSE Africa-Eurasia convergence (Di Bucci et al., 2010).

The shear zones in AD4 have been active at least since the Mesozoic (de Alteriis, 1995; Argnani et al., 1993; Colantoni et al., 1990; De' Dominicis and Mazzoldi, 1987; Morelli, 2002; Tramontana et al., 1995), and are inherited from earlier Adria microplate deformation stages (Anderson, 1987; Anderson and Jackson, 1987; Catalano et al., 2001; Channell et al., 1979; Wortmann et al., 2001). The degree of knowledge for each fault system varies, depending on 1) subsurface information from published (Morelli, 2002; VIDEPI, 2010) and unpublished (Fracassi et al., 2004, 2006) data that reached into the Apulian platform and below, and 2) seismological (historical or instrumental), field, paleoseismological (including marine one), and geochemical evidence. More information is available for the southern sector of AD4, where both seismicity and field evidence are easier to investigate (the latter being at times debated in the literature; i.e., Billi, 2003; Billi et al., 2007; Brozzetti et al., 2006; Piccardi, 2005; Tondi et al. 2005). In contrast, the northern sector of AD4 is more complex, available evidence is more elusive and resorting to regional seismotectonic models is necessary to address puzzling earthquakes such as the Mw 6.0 sub-event of the 30 December 1456 seismic sequence and the 5 September 1950, Mw 5.7 Gran Sasso event. The regional approach rests largely on the views expressed by Fracassi and Valensise (2007).

The occurrence of the 31 October and 1 November 2002 Molise twin earthquakes (both Mw 5.8) has had an intense impact on the seismological understanding of the moderate earthquakes that affect the Adriatic side of the Apennines belt and on the interpretation of the deep-seated, E-W trending shear zones seismogenic potential (Di Bucci and Mazzoli, 2003; Di Bucci et al., 2006; Di Luccio et al., 2005; Fracassi and Valensise, 2007; Latorre et al., 2010; Valensise et al., 2004). These events have also shed new light onto less known historical earthquakes that had occurred farther to the east, well within the Adriatic foreland. Besides posing compelling questions to the geologist seeking field evidence for an unexpectedly deep sequence, the 2002 earthquakes eventually led to reevaluation of the adjacent 30 July 1627, Mw 6.7, Gargano event, for which also strong tsunami effects are reported (Boschi et al., 1995; De Martini et al., 2003; Guidoboni and Comastri, 2005; Guidoboni et al., 2007; Paulatto et al., 2007; Pasarić et al., 2012; Tinti et al., 1995), despite its inland occurrence (Rovida et al., 2011).

Historical and instrumental catalogues (Castello et al., 2006; Guidoboni et al., 2007; ISIDe, 2010; Rovida et al., 2011) and selected studies (Guidoboni and Comastri, 2005; Fracassi and Valensise, 2007) show that only two key earthquakes have affected the northern part of AD4; the 5 September

1950, Mw 5.7 and the northernmost earthquake of the 30 December 1456, Mw 6.0, seismic sequence. Elsewhere, the coastal and offshore sector of northern AD4 appears to be almost ‘seismically silent’, with sparse low-energy seismicity inland (Del Gaudio et al., 2001, 2005, 2007), whereas significant earthquakes have affected its southern and south-eastern sector, culminating with the 30 July 1627, Mw 6.7, Gargano earthquake. The reassessment of smaller earthquakes, such as the Gargano 31 May 1646, Mw 6.6 and the 29 January 1657, Mw 6.4 (Camassi et al., 2008) led to a reconsideration of the seismogenic potential of the entire region and triggered the quest for their sources.

Focal mechanisms (Frepoli and Amato, 1997; Gasparini et al., 1985; Pondrelli et al., 2006; Herrmann and Malagnini, 2011; Pondrelli et al., 2011) are available primarily for the southern sector of AD4 and show prevailing right-lateral, strike-slip deformation (Figure 1c).

Three earthquake-induced tsunamis were reported for AD4 (Pasarić et al., 2012; NOAA/WDC Tsunami Database), the key one being that associated with the 30 July 1627, Mw 6.7 earthquake, bearing $I = 5$ (very strong), according to the Sieberg-Ambraseys scale (Ambraseys, 1962). Recall that, as remarked earlier in this paragraph, the location of the 1627 earthquake is well inland.

GPS data in AD4 show a self-consistent pattern of NNE-SSW trending horizontal velocities in the range of 3.0 to 4.0 mm/yr with respect to a fixed Eurasia (D’Agostino et al., 2008; Devoti et al., 2008, 2011). In the northern and central sector of AD4, the orientation of GPS vectors are in agreement with orientation of active stress (Heidbach et al., 2010) and borehole breakout data (Montone et al., 2012). Towards the eastern Gargano promontory, maximum horizontal stress vectors trend progressively WSW-ENE. The InSAR data by Atzori et al. (2007) suggest that the northern portion of the Gargano promontory is being uplifted with respect to the portion south of the Mattinata Fault.

From northwest to southeast in AD4 we identify six CSSs (ITCS075, ITCS059, ITCS003, ITCS058, ITCS070, ITCS074) and nine ISSs (ITIS096, ITIS094, ITIS053, ITIS052, ITIS022, ITIS021, ITIS020 and ITIS133). Details on the sources are supplied in Figure 6, along with a list of earthquakes with $M_w > 5.5$ and the associated tsunami.

The ITCS075 source belongs to the Northern Abruzzo shear zone. It straddles the northeastern piedmont of the Abruzzo region between L’Aquila to the west and Pescara and its offshore to the east (Figures 1a and 6). In our view this source is the northernmost expression of the oblique to right-lateral strike-slip reactivation that is affecting the deep-seated, inherited shear zones in the central and southern Adriatic foreland. The source is a near-vertical, S-dipping fault system lying below the outer Apennines thrusts and located just east of the main extensional axis of the central-southern Apennines. Seismicity for this source is scarce, but a key Mw 5.7 earthquake ruptured the westernmost portion of this source on 5 September 1950. Field evidence for this source is also scarce, while subsurface data (see Scisciani et al., 2001) suggest the presence of a ca. E-W trending deep-seated, blind set of sub-vertical structures whose westernmost portion (ITIS096) has been associated with the 1950 earthquake (Basili et al., 2008).

The ITCS059 Source, belonging to the Tremiti Line, is in part based on the “Tremiti lithospheric tear” (Doglioni et al., 1994; Scrocca et al., 2007), or “Tremiti Line” (auct.). This source crosses the piedmont of the Abruzzo region south of Pescara (Figures 1a and 6), from west to east toward the Tremiti Islands, located about 25 km N of the Gargano promontory. The source is a near-vertical, S-dipping, fault system located to the east of the main extensional axis of the central-southern Apennines. According to historical and instrumental catalogs (Guidoboni et al., 2007; Pondrelli et al., 2006; Pondrelli et al., 2011; Rovida et al., 2011), seismicity is very limited. However, based on the data by Guidoboni and Comastri (2005), Fracassi and Valensise (2007) maintain that a sub-event of the 30 December 1456 multiple earthquake has ruptured a portion of this source near its

western end. This source is a long strike-slip, right-lateral fault system that is thought to run ca. E-W across the Apulian domain. Field evidence in the area is relatively scarce in the western sector of this source. Geochemical anomalies and radon leakage in the Vasto High (Ciotoli et al., 2004, 2006) and the E-W reactivation of inherited faults in the Tremiti Islands. (Brozzetti et al., 2006), however, hint at a deep-seated (rooting at ca. 20 km) set of blind structures.

The ITCS058 Source is part of the Molise-Gondola shear zone (Di Bucci et al., 2006). It includes fault segments that have been investigated (Piccardi, 2005; Tondi et al., 2005; Billi et al., 2007) based on field evidence of recent deformation along exposed portions of the Mattinata Fault, a large tectonic feature crossing the Gargano promontory from west to east (see Argnani et al., 2009 and references therein). In fact, several earthquakes with magnitude up to 6.0 are reported for the entire area encircling the Gargano promontory (Boschi et al., 1995; Console et al., 1993; Gruppo di lavoro CPTI04, 2004; Guidoboni et al., 2007; Milano et al., 2005; Rovida et al., 2011).

The ITCS070 and ITCS074 Sources can be considered the offshore portion of the Mattinata Fault. This sector has commonly been known as the Gondola Ridge or Gondola Fault (Argnani et al., 1993; Colantoni et al., 1990; de Alteriis and Aiello, 1993; De' Dominicis and Mazzoldi, 1987; Morelli, 2002; Tramontana et al., 1995). The Gondola Fault has long been considered an inactive, long-lived, inherited contractional feature of the Adriatic foreland. Recently, very high resolution seismic data (Di Bucci et al., 2009; Ridente and Trincardi, 2006; Ridente et al., 2008a, 2008b) have shown evidence of current tectonic activity for ca. 50 km east of the eastern tip of the Mattinata Fault. Fracassi et al. (2012) have proposed that the western segment of the Gondola Fault zone is a potential seismogenic source of the 10 August 1893, Mw 5.4 earthquake, currently located just along the Gargano shore (Gruppo di lavoro CPTI04; Rovida et al., 2011). Also notice that Baratta (1894) reported slight tsunami effects associated with the 10 August 1893, Mw 5.4, earthquake that occurred at the eastern tip of the Gargano promontory.

4.5. Central Western Adriatic – AD5

The Central Western Adriatic region (AD5) includes the structural unit of the external Central-Northern Apennines thrust belt. It spans about 260 km along the Western Adriatic coastline between the latitude of the cities of Rimini (to the north) and Pescara (to the south) and widens up to ca. 35 km across the belt. The composite sources included in AD5 straddle the entire Adriatic coastal sector and the offshore of the Emilia Romagna, Marche, and Abruzzo regions.

For the external portion of the Northern and Central Apennines DISS lists two parallel, about 260 km-long, fault systems, broken down into eight CSSs (Figure 7), each including at maximum four individual sources. Overall AD5 includes 10 ISSs.

In the literature much of the tectonic activity in AD5 is distributed between the so called "transverse structures", i.e. NE-SW-trending, sub-vertical faults characterised by unclear kinematics, and the thrust-faults driving of the Apennines belt. The "transverse structures" may thus represent tear faults that accommodate strain between different thrust-fault segments, but to date the seismogenic potential of these structures is yet to be ascertained. AD5 is bordered to the north and to the south by the transverse structures of Arbia-Val Marecchia Line and the Tremiti Line, respectively (Figure 1b). Both are two of the most important tectonic transverse inherited lineaments of the whole Apennines. The Arbia-Val Marecchia Line is a strike-slip fault system active since the Tortonian (e.g. Boccaletti et al., 1977; Ricci Lucchi, 1975; Servizio Geologico d'Italia, in press, and references therein), while the Tremiti Line is a lithospheric right-lateral transfer zone, already described in AD4. The location of the youngest structures in the outermost portion of the northern and central Apennines thrust systems coincides with a significant peak of seismic moment released

by instrumental and historical earthquakes (Basili and Barba, 2007; Chiarabba et al., 2005; Rovida et al., 2011). These fronts are E-verging fault systems running nearly parallel to the Italian coastline. The geometry of the main thrusts is well-known having been described in classical studies (e.g., Argnani et al., 1991; see also Barchi, 2010 for a review). Recently, Scrocca (2006), and Scrocca et al. (2007) proposed a more external position for the outermost Apennines thrust front in the Central Adriatic domain. Apart from some conflicting interpretations regarding the thrust system architecture, the timing of the end of the contractional deformations is still debated. Coward et al. (1999) and Di Bucci and Mazzoli (2002) proposed that thrusting and related folding in this area ceased in the Early Pleistocene, whereas the presence of compressional seismogenic sources all along the front of the northern-central Apennines, has been proposed by other researchers (e.g., Basili et al., 2007; Burrato et al., 2003; Vannoli et al., 2004; Wegmann and Pazzaglia, 2009).

The prevailing structural elements of the external Apennines are E-verging thrust faults and their associated anticlines. The strike of these structures is NW-SE in the Rimini - Ancona sector and about N-S from Ancona to Pescara (Figure 1a), with the change in strike occurring at the well-known Olevano-Antrodoco-Sibillini Line (Figure 1b) transverse (Calamita et al., 2011 and references therein). This NNE-striking inherited lineament: 1) bounds different paleogeographic domains; 2) separates the Abruzzi extensional domain from the Alto Tiberina normal fault system (Boncio et al., 2000); and 3) marks a change in the dip direction of the master seismogenic fault systems (Vannoli et al., 2012, and references therein). Nevertheless the role and degree of activity of the Olevano-Antrodoco-Sibillini Line is still widely debated in the literature.

The Umbria-Marche region was thoroughly investigated using seismic reflection profiles, and different interpretations of its structural style are available in the literature. The main differences concern the position of the basal decollement of the thrusts, and the presence or absence of secondary shallower decollement levels. Some researchers (Bally et al., 1986; Doglioni et al., 1994) indicate the bottom of the Triassic evaporites as the basal decollement level, and propose that a thin-skinned tectonics has characterized the Paleogene-Neogene evolution of the belt. Other investigators (Barchi et al., 1998a; Butler et al., 2004; Finetti et al., 2001; Lavecchia et al., 2003) consider that also the upper portion of the basement was involved in thrusting, and propose a thick-skinned structural style. In general there is good agreement among the researches (e.g.: Barchi et al., 1998a; Coward et al., 1999; Calamita et al., 1994) about the presence of two main decollement levels inside the accretionary prism, the lower one coinciding with the bottom of the Triassic evaporites, from which the major thrust ramps originate and the shallower one coinciding with the Marne a Fucoidi or Scaglia Cinerea formation, from which minor thrust planes detach. Thus, the deformation style of the Umbria-Marche region is characterized by two main structural levels: 1) a lower one, consisting of deep (down to 6-10 km depths) and broad (wavelengths of 5-10 km) anticlines deforming the Mesozoic-Paleogene carbonate succession, produced by major thrust ramps detaching from the Triassic evaporites (Umbria-Marche folds); and 2) a shallower level, consisting of small scale, short wavelength anticlines detached at 2 km depth, present in the axial zones of the major anticlines, and developed in the Neogene foredeep sediments. The latter anticlines show a more complex structural pattern with respect to the deeper ones. In summary, the geometrical features of AD5 are: 1) the occurrence of complex thrust trajectories due to the presence of several potential detachment levels in the sedimentary multilayer; 2) upward decreasing in the anticlines wavelength; and 3) disharmony between different structural levels.

GPS data available for AD5 display a general NE-SW trend of horizontal velocities with respect to fixed Eurasia, showing a clear compressional regime (D'Agostino et al., 2008; 2011; Devoti et al., 2008; 2011). In the northern part of AD5 these data agree with borehole breakout data (Heidbach et al., 2010; Montone et al., 2012) that also show a compressional tectonic regime with a maximum

horizontal stress axis rotating from N-S in the Po Plain to NE-SW along the Adriatic coast, following the trend of the main Apennines fronts. In the southern part of AD5 borehole breakout data are more ambiguous and give rise to contrasting views (Heidbach et al., 2010; Montone et al., 2012). Basili and Barba (2007) also describe active compression in the Northern Apennines and quantify long-term migration and shortening rates of 8.85 ± 0.61 mm/yr and 2.93 ± 0.31 mm/yr, respectively, through an original statistical treatment of structural and tectonic data.

Historical and instrumental catalogues (Castello et al., 2006; Guidoboni et al., 2007; Rovida et al., 2011) show that numerous damaging earthquakes have occurred onshore and offshore, especially in the northernmost portion of AD5, whereas to the south seismicity is low along the entire length of the belt. Strong earthquakes include, from north to south, the 17 May 1916, Mw 6.0 and 16 August 1916, Mw 6.1, Alto Adriatico events; the 30 October 1930, Mw 5.8, Senigallia event; and the 3 October 1943, Mw 5.8, Offida event. The latter event had the largest epicentral intensity (I=VIII-IX). In 1916, a long seismic sequence started on 17 May (Mw 6.0) and lasted until December, causing intensity VIII damage in Rimini and neighbouring towns (Guidoboni et al., 2007; Locati et al., 2011). The first large shock occurred on 17 May, but the two shocks of 16 August (Mw 6.1 and 5.5) worsened the damage. The earthquakes hit Rimini and the coastal localities particularly hard, although their macroseismic location is offshore (Rovida et al., 2011).

Focal mechanisms (Frepoli and Amato, 1997; Gasparini et al., 1985; Pondrelli et al., 2006; 2011; Santini, 2003) and structural geology data show that reverse, oblique and strike-slip motion are the prevailing modes of seismic deformation in AD5, with a homogeneous stress field characterized by horizontal compression oriented NE-SW (Frepoli and Amato, 2000).

The focal solutions of the 2000, Faenza seismic sequence, that occurred 60 km northwest of Rimini, show NE-SW horizontal compression for the main events (Mw 4.9; Calderoni et al., 2009; Pondrelli et al., 2006). Moreover, in the southern part of AD5, 50 km south of Ancona, the focal mechanisms for the 1987, Porto San Giorgio earthquake (Mw 5.1) show NE-SW horizontal compression (Riguzzi et al., 1989). Between January and February 2010, a compressional sequence at a depth of about 20 km and with maximum Mw of 4.0 hit the southern Marche (ISIDe, 2010; Hermann et al., 2011).

Several earthquake-induced historical tsunami flooded the Adriatic coastline of AD5 (Boschi et al., 1995; for a summary see Table 1 in Vannoli et al., 2004) all located in the northern part of the region. Tinti et al. (2004) included in their database only two of these tsunami, while Pasarić et al. (2012), following the revision of Maramai et al. (2007), present in their database four events for AD5 (Figure 7). The strongest tsunami rated I 4 (strong) according to the Sieberg-Ambraseys scale (Ambraseys, 1962) was the October 1930 event that flooded the Ancona harbour following the 1930 earthquake. Contemporary newspapers reported that a sudden high tide was noticed and the sea “boiled”. An American steamship broke its mooring, was slammed against the dock and suffered heavy damage. The docks were heavily damaged too (Boschi et al., 1995; Maramai et al., 2007).

In AD5 we identify eight CSSs (ITCS039, ITCS030, ITCS032, ITCS043, ITCS008, ITCS031, ITCS020, ITCS054) and ten ISSs (ITIS036, ITIS035, ITIS034, ITIS033, ITIS032, ITIS031, ITIS024, ITIS030, ITIS029, ITIS070). All sources are shown in Figure 7 and at the western end of the three geological sections of Figure 2.

The prevailing strike of these sources is NW-SE in the northern area, from Cesena to Ancona, and about N-S in the southern area, from Ancona to Pescara. The strike of these sources was based on that of the mapped regional structures and/or on the seismic reflection profiles. All sources strike

roughly parallel to the coast and are E-verging, as are the seismogenic fault systems at the eastern border of the Apennines chain (Figure 2). The dip angles and the minimum and maximum depth were based on subsurface data and geometrical considerations on thrust geometries. All sources in AD5 locate within the upper crust, with a maximum depth of 9.0 km for the ITCS020 source. Subsurface data well image onshore and offshore anticlines whose growth is caused by the eastward advancing thrusts. Therefore, the geometry of these seismogenic sources has been investigated by integrating the interpretation of available well data and seismic reflection profiles (Bally et al., 1986; Barchi et al., 1998a, 1998b; Calamita et al., 1991, Calamita et al., 1994; Cuffaro et al., 2010; Fantoni and Franciosi, 2010; Scisciani et al., 2002; Scrocca et al., 2003; Scrocca et al., 2007; ViDEPI, 2010).

Blind thrusting has been recognized as the tectonic mechanism responsible for the seismogenic faulting style of AD5, therefore, the rake is always assumed to reflect pure compressional faulting. The slip rates were based on geological data or inferred from geological observations in adjacent structures that share the same tectonic environment and fall in the 0.10–0.50 mm/yr range. The M_{max} was assigned based on seismic catalogues and on the geometric characteristics of the sources. The largest value (M_w 6.1) was assigned to the ITCS030, ITCS032, and ITIS031 sources; all other sources of AD5 were assigned a M_{max} ranging between 5.5 and 5.9.

Some of the ISSs of AD5 belonging to the ITCS032 Pesaro-Senigallia Source are described below; for an in-depth analysis of these and other seismogenic sources the reader may refer to the DISS website, <http://diss.rm.ingv.it/diss/>. Complete parameters for the CSSs and ISSs of AD5 are supplied in Figure 7.

The coastal area north of Ancona is presently affected only by low seismic activity, but damaging earthquakes struck this area in the recent past, e.g. the 30 October 1930, M_w 5.8, Senigallia earthquake. The main tectonic structures of this sector are the so called “Coastal Anticlines” (Barchi et al., 1998a; Nanni and Vivalda, 1987) that are growing folds (e.g. Basili et al., 2007) whose inception age and activity rate were studied by means of syn-tectonic deposits analysis (Basili and Barba, 2007). The occurrence of a sizable tsunami following the 1930 earthquake (Boschi et al., 1995; Maramai et al., 2007; Pasarić et al., 2012) suggests that the source is very near to the coast or offshore and has been able to produce significant vertical displacement of the sea floor. Vannoli et al. (2004) performing a geomorphological analysis of tectonically warped and tilted river and coastal terraces and of drainage anomalies, suggested that deformation of the coastal area from Rimini to Ancona is due to active blind thrusts driving the growth of the coastal anticlines. According to this study, these structures are responsible for the largest earthquakes in the region (e.g. 1930 event) and move at a slip rate of 0.24 - 0.36 mm/yr. The same study was the base for constraining the ITIS030 Source parameters associated with the 1930 earthquake. In particular, the geometry and width of the fault is based on a seismic reflection profile by Bally et al. (1986) and its length is constrained on the basis of the wavelength of the major fluctuations of the fold axial-plane. The study by Vannoli et al. (2004) considers the entire Northern Apennines front up to Rimini active and treats the individual thrust segments as potentially seismogenic even if they are not associated with strong (i.e. $M > 5.5$) recorded earthquakes. Following this reasoning, the DISS database includes also the ITIS031 and ITIS032 Sources, segments of the coastal anticlines. Since these Sources are not associated with any earthquake, they can be regarded as “seismic gaps”.

5. DISCUSSION

Working in the Adriatic domain poses significant challenges in the identification of seismogenic sources since most of the area is covered by the sea. This circumstance must be taken into consideration when evaluating the reliability of the input data of our model.

A critical issue for the region presented in this study is that it belongs to different countries that have a different history of research activities and data accessibility. For this study we retrieved and standardized all available seismological and geological material from both sides of the Adriatic Sea and obtained an integrated model of seismogenic sources for the whole Adriatic domain. Most of the sources belong to "relatively low seismicity" areas, especially in the northern Adriatic domain, where significant earthquakes are less frequent with respect to its southern counterpart and the magnitude is generally < 6.0 . The sources of infrequent moderate-size earthquakes may have a limited surface expression and hence be very difficult to be identified geologically. However, we stress the importance of including also the more seismically "quiet" sources in a comprehensive seismogenic model as they may pose a significant hazard to critical facilities (e.g. Slejko et al., 2011).

Combining different data types may introduce ambiguous solutions when determining the parameters of seismogenic sources and characterizing their behavior. A good example of these ambiguities is supplied by the combination of seismic reflection and earthquake data for the HRCS020 Source. Available interpretations of the seismic profile (Fantoni and Franciosi, 2010; Grandić and Markulin, 2000; Grandić et al., 2004) all show the presence of deep seated, steeply-dipping faults arranged in a positive flower-type geometry (see profile 3, Figure 2). In the interpretation of Grandić and Markulin (2000) and Grandić et al. (2004) such faults stop at a minimum depth of about 7 km and do not affect the shallowest portion of the crust. They show evidence of up-dip displacement, while their inherited geometry is compatible with their older extensional character. In contrast, Fantoni and Franciosi (2010) show the prolongation of these faults into the uppermost crust, where they produce anticlines in Mesozoic carbonates and cut through Neogene rocks. Their interpretation also assigned a more gentle dip to these faults and shows intermediate dip thrusts branching off subvertical deep-seated faults. Available observations for the 2003 Jabuka earthquake sequence (Herak et al., 2005; Pondrelli et al., 2006; Global CMT Catalogue) show a WNW-ESE trend for the seismic sequence with each individual event having a WNW-ESE to E-W oriented fault plane dipping at an intermediate angle. The HRCS020 Source, together with the corresponding individual HRIS001, represents the seismically active thrust plane located in the 2 - 12 km depth and dipping towards the ENE at an intermediate angle (Figure 2). Besides proposing a different geometry with respect to the interpretations of seismic reflection data, our interpretation implies that the HRCS020 belongs to the External Dinarides thrust belt. The HRCS020 Source is in agreement with the interpretation proposed for the western Central Adriatic by Scrocca et al. (2007), who contend that the early compressional phase caused the inversion of extensional faults while in the Plio-Quaternary active thrusting along low- to mid-angle faults is superimposed on the basement-involving normal faults.

A further example of contradicting data was encountered during the parameterization of the HRCS008 Source. Seismic reflection data (Fantoni and Franciosi, 2010; Grandić and Markulin, 2000; Grandić et al., 2004; Tari, 2002) show a different structural and geometrical interpretation of the Dugi Otok fault, the parent fault of HRCS008. In their study, Grandić and Markulin (2000) show a low- to mid-angle thrust fault that is underlain by an older but potentially reactivated normal fault. Grandić et al. (2004) represented the Dugi Otok fault as one of a series of shallow fault splays dying out on a decollement above 10 km depth, while Fantoni and Franciosi (2010) described the Dugi Otok fault as one of the leading fault splays rooting into the decollement around 10 km depth.

Both interpretations show the presence of a steeply dipping underlying fault located within the Variscan basin. A further interpretation is supplied by Tari (2002), who considers the Dugi Otok fault as the main thrust fault extending from very shallow depth down into the lower crust. Such interpretation is supported by the seismotectonic work of Kuk et al. (2000), who described a single deformation zone with moderate dip extending from the sea bottom to 20 km depth and corresponding to the Dugi Otok fault. Our HRCS008 Source describes a mid-angle thrust dipping towards the NE and located in the depth interval 2-18 km as representative of the seismically active part of the Dugi Otok fault.

Uneven data availability, diverse interpretations of available seismic data, and conflicts between seismic reflection and earthquake data allow for different interpretations of the current structural setting of the Central Adriatic (e.g. Grandić and Markulin et al., 2000; Herak et al., 2005; Scisciani and Calamita, 2009; Scrocca, 2006). Our interpretation of the seismogenic sources of the Central Adriatic shows that the external thrusts of the Apennines and External Dinarides lie next to each other along the ITCS052 and HRCS14 Sources. Such interpretation shows that the thrust belts currently occupy what used to be the foredeep area of both thrust belts. Through the CSSs (Figures 2 and 5) we map the leading SW and NE dipping thrust planes responsible for the release of the seismic deformation. We do not include in our model the smaller scale fault planes arranged in a reverse horst geometry with opposite dip direction proposed by Scisciani and Calamita (2009), because 1) such planes cross-cut each other at depth, 2) they are too small to host a $M_w \geq 5.5$ earthquake, and 3) are generally not in accordance with earthquake data.

The vast majority of sources in the Adriatic domain have a NW-SE trend and thrust/reverse kinematics (Figures 8a and 9). The exceptions to these characteristics are the E-W oriented dextral strike-slip faults of the Southern Central Adriatic (AD4). These sources are subvertical to vertical faults occurring in the depth range 6-25 km. The only exceptions are the deep-seated ITCS058 and ITCS074 that are presumed to be surface breaking. In the case of ITCS070 and ITCS074 the sources are arranged in a vertically segmented structure, where the deeper portion of the fault (ITCS070) has as pure dextral strike-slip kinematics, while the upper portion (ITCS074) displays oblique tectonics with a slight extensional component. The sources in the southeastern portion of AD2 region display the lowest dip angles among all sources in the Adriatic domain. In the Eastern Adriatic (AD1 and AD2) the most internal sources exhibit steeper dip angles with respect to sources located closer to the outer front. In addition, the most internal sources (ITCS100 and HRCS032 in AD1) exhibit a rather large strike slip component, while the most external ones are purely reverse (ITCS101 and HRCS029 in AD1).

A slight variation from the regional NW-SE trend is seen for the WNW-ESE trending HRCS002 and HRCS008. These sources, along with HRCS018, display deeper seismogenic depths and a slight left lateral strike-slip component. The largest depths, not considering sources of AD4, are found for HRCS005 and HRCS008 that are interpreted to be the main active faults in their respective areas. In contrast, sources in AD5 exhibit the shallowest depths and are interpreted as thrust splays branching off a shallow decollement. The sources that are thought to be able to generate the strongest earthquakes in the region ($M \geq 7$) are MECS001 and HRCS001, located in the southern portion of the Eastern Adriatic (Figure 8b). The geometry and seismogenic depth of both of these sources is compatible with $M \geq 7$ earthquakes, both having a record of $M_w \geq 7$ earthquakes. Sources capable of generating earthquakes up to $M 6.5$ are mainly those of the Eastern Adriatic that exhibit deeper seismogenic depths and larger width. The exceptions are the smaller fault splays and the HRCS007 and HRCS018 sources, that have a $M_w 5.8$ assigned as their maximum magnitude. Sources of the Central Adriatic are not expected to exceed $M_w 6.5$, while sources of AD5 should not exceed $M_w 6.0$ with the only exception of ITCS030 and ITCS032.

Sources of AD4 exhibit a large variability in terms of M_{max} , ranging from the lower magnitude range of 5.5 (ITCS070) to 6.7 (ITCS003).

M_{max} values for our sources are generally in a good agreement with the historical and instrumental record (Shebalin, 1974; Herak et al., 1995; Gruppo di lavoro CPTI, 2004; Papazachos et al., 2009; Thessaloniki Macroseismic Database, 2010; Rovida et al., 2011). The region displaying the largest disagreement between assigned and observed M_{max} is AD1. The largest earthquake associated with sources of this region is the 14 August 1574, Lupoglav earthquake, whose inferred magnitude is M_w 5.6, in contrast with the 6.5 M_{max} we set for its presumed causative source. The reason for this arises from consideration of the source geometries, their seismogenic depths and thus their capability to generate larger earthquakes. Such decision is supported also by the observation that, although no earthquake larger than M_w 5.6 is associated with AD1 sources (Rovida et al., 2011), those sources that lie to the southeast and are the structural prolongation of AD1 sources are associated with stronger earthquakes – namely the 1323, M_w 6.0 Novi Vinodolski earthquake (Rovida et al., 2011).

The slip rate we assigned to seismogenic sources is expressed as an interval; slip rates are then subdivided in classes to better represent their variability (Fig 8c and 8d). Sources of the Central Adriatic (AD3) have the lowest minimum slip rates (< 0.10 mm/yr). All of the rest of the Adriatic domain sources have minimum slip rates in the range 0.10 to 0.50 mm/yr, except for MECS001 that has the minimum slip rate ranging between 0.5 and 1.0 mm/yr. The lowest maximum slip rates (range of 0.10 - 0.50 mm/yr) are typical of Central Adriatic sources (except for ITCS052), as well as for AD1 sources and for the northwesternmost (HRCS005, HRCS025) and more internal (HRCS013, HRCS015) sources of AD2. The most frequent maximum slip rate range for the Adriatic domain sources is 0.5 - 1.0 mm/yr. These values are typical of thrusts in AD5, of some thrusts in AD2, and of some strike-slip sources in AD4. The largest maximum slip rates are typical of the southern parts of the Adriatic domain; the maximum slip rate for the ITCS058, ITCS059, ITCS074, HRCS002, HRCS001, HRCS016 and MECS007 sources falls in the range 1.0 - 1.5 mm/yr, while for MECS001 the range is 1.5 - 2.0 mm/yr. Sources in AD1 show very little or no variability between their minimum and maximum slip rate values as both values fall within the 0.1 - 0.5 mm/yr range. The same is true for the most internal sources of AD2 (HRCS013, HRCS015). Minimum and maximum slip rate most commonly varies of one class (Figure 8c and 8d). The largest variability of two interval ranges is seen for the sources that have larger maximum slip rates; ITCS058, ITCS059, ITCS074, HRCS002, HRCS001, HRCS016, MEC001 and MECS007.

The smallest slip rates are typical of sources located in the Central Adriatic (AD3). The Adria lithosphere is 1.0 - 1.5 orders of magnitude more resistant to deformation than its margins (Tesauro et al., 2009; Carafa and Barba, 2011). The rigidity of the Adria lithosphere seems to reflect also in the lower slip rates relative to regions with lesser strength.

Sources located in the southern Adriatic domain have higher slip rates with respect to the sources located in its northern part. Fault kinematics does not seem to play a role on determining slip rate, although the results obtained might indicate that thrust faults are more efficient in accommodating the regional velocity field in the form of fault slip with respect to the strike slip faults. The comparison between slip rates and maximum magnitude does not show important patterns with the exception that sources with largest maximum magnitude are generally also those with the biggest maximum slip rates. The opposite cannot be said, as also slow moving sources are thought to be able to generate strong earthquakes.

Slip rates for the Eastern Adriatic were calculated through a finite element modeling technique and compared with other available values (see Kastelic and Carafa, 2012), whereas slip rates for the

Western Adriatic were derived from displaced geomorphic markers (Vannoli et al., 2004) and estimated from regional geological and geodynamic considerations. The ongoing reassessment of slip rates using 3D geological modelling in part of our AD5 is expected to provide better constraints for fault activity (Maesano et al., this issue). We are aware that slip rate values of seismogenic sources are affected by uncertainties related to the different methodologies used to calculate and estimate them and that they do cover different time scales. Despite these constraints, the slip rates presented here for sources of the Adriatic domain are all based on either available or original data and are a useful indication of slip rate characteristics and variability throughout the region.

Our model inevitably suffers from uncertainties in the input data. This is mainly due to the offshore location of most of the faults and to limitations of the methodologies used for their identification. One of the biggest challenges was setting the maximum depth. Seismic reflection data may provide ambiguous estimates, while earthquake hypocentral depths suffer from uncertainties due to sparseness of the networks and large epicentral distances from seismometric stations, when these belong to the same network – not always the case in the Adriatic domain. We contend that by combining various datasets and further analyzing them we captured well the geometry and the seismogenic depth of the sources, and that future new data and more precise interpretations will improve our model, particularly for what concerns the geometry of the offshore structures. A good example of these circumstances is the outermost Apennines thrust in the northern Adriatic Sea shown in Section 2 of Figure 2. An older interpretation of this structure envisaged this thrust as detaching at shallow depth (e.g. Bally et al., 1986), which implies a limited seismogenic potential. Therefore, this shallow thrust was not included in previous versions of the DISS database. The new interpretation by Fantoni and Franciosi (2010) shows a deeper level of decollement, hence a larger fault plane capable of generating sizable earthquakes (e.g. $M_w > 5.5$). These new characteristics turned this structure into a candidate for inclusion in the DISS after careful revision of its most recent activity.

Based on the characteristics of our sources, we divided the Adriatic domain into five seismotectonic regions (Figure 9). Three of them correspond to the active part of the Central - Northern Apennines, Eastern Southern Alps and External Dinarides, all verging towards the Adriatic domain. A dextral strike-slip corridor characterizes the transition zone between the Southern Alps and the External Dinarides in W Slovenia. A region of active dextral strike-slip deformation also affects the Southwestern Adriatic. Here, strike slip faulting affects different crustal levels with a minimum faulting depth becoming deeper westwards, where the strike slip faulting coexists with active thrusting in the shallow crust. As seen in Figure 9, the AD5 Apennines and the AD4 dextral strike-slip domains partially intersect in map view. Such setting is due to different depth interval of seismogenic sources in both domains. Thrust faults in the southern part of the AD5 affect the depth interval between three and nine kilometres, while the northern based dextral strike-slip faults of AD4 lie below in the depth interval between 11 and 20 kilometres.

Fully parameterized and internally consistent ISSs and CSSs can be used as input data for further analyses. By characterizing the geometrical, kinematic and activity parameters of each source, we supplied parameterized geological information for active faults to be used in seismic and tsunami hazard calculations, geodynamic modeling, calculation of ground shaking scenarios and various other applications. We stress that most of these applications will benefit from both the availability of homogeneously parameterized source characteristics and of the estimates of the uncertainties associated with each parameter.

6. CONCLUSIONS

We presented a seismogenic source model for the Adriatic domain. This work supplies a detailed and in-depth characterization of the seismogenic sources responsible for strong and moderate earthquakes of this region. All sources are identified and characterized by their geometrical, kinematic and activity parameters using common criteria to ensure and the homogenization of the model and to grant direct comparison among them. The model hence supplies a synoptic view of active faulting and of the modes of seismic release in the whole Adriatic domain. Moreover, the model supplies new data that can be integrated into studies for the evaluation of the earthquake and tsunami hazard in the region.

The Adriatic domain is largely characterized by NW-SE thrusts, with the notable exception of the dextral strike-slip sources of AD4 which, in addition to displaying a different faulting style, occur at deeper crustal depth and exhibit a distinct E-W trend.

Sources of the southern portion of the Adriatic domain display the largest slip rates, while those in the Central Adriatic region (AD3) are the slowest. The southeasternmost sources of the Eastern Adriatic region (AD2) display the largest expected maximum magnitude, while the sources with the lowest maximum magnitude are those of the Central Western Adriatic region (AD5).

The characterization of Composite and Individual Seismogenic Sources by studying fault properties, seismic sequences, deformation patterns and geomorphology may help identifying potential seismic gaps; faults that show geological evidence of recent activity and belong to a system of seismically active faults but have not yet hosted an historical or instrumental earthquake can thus be singled out for further consideration. During our reassessment we have identified the ITIS031 and ITIS032 sources as potential seismic gaps within the Adriatic domain, but others may exist in areas where geological and historical information is still too sparse.

REFERENCES

- Akinci, A., Galadini, F., Pantosti, D., Petersen, M., Malagnini, L., Perkins, D., 2009. Effect of time dependence on probabilistic seismic-hazard maps and deaggregation for the Central Apennines, Italy, *Bulletin of the Seismological Society of America*, 99, 2A, 585–610, doi: 10.1785/0120080053.
- Akinci, A., Perkins, D., Lombardi, A., Basili, R., 2010. Uncertainties in probability of occurrence of strong earthquakes for fault sources in the Central Apennines, Italy. *Journal of Seismology* 14, 95–117, doi: 10.1007/s10950-008-9142-y.
- Allen, P.A., Homewood, P., Williams, G.D., 1986. Foreland basins: an introduction, in: Allen, P.A., Homewood, P. (Eds.), *Foreland Basins*. Int. Ass. Sed. Special Publication 8, 3-12.
- Ambraseys, N. N., 1962. Data for the investigation of the seismic sea-waves in the Eastern Mediterranean. *Bulletin of the Seismological Society of America* 52, 895-913.
- Anderson, H., 1987. Is the Adriatic an African promontory? *Geology* 15, 3, 212–215, doi: 10.1130/0091-7613(1987)15<212:ITAAAP>2.0.- CO;2.
- Anderson, H., Jackson, J., 1987. Active tectonics of the Adriatic region. *Geophysical Journal of the Royal Astronomical Society* 91, 937–983, doi 10.1111/j.1365- 246X.1987.tb01675.x.
- Advanced National Seismic System (ANSS) Composite Earthquake Catalog, Northern California Earthquake Data Center, <http://quake.geo.berkeley.edu/cnss/>, last accessed 2 March 2012.
- Argnani, A., Artoni, A., Ori, G., Roveri, M., 1991. L'avanfossa centro-adriatica: stili strutturali e sedimentazione. *Studi Geol Camerti* 1991/1, 371–381.
- Argnani, A., Favali, P., Frugoni, F., Gasperini, M., Ligi, M., Marani, M., Mattiotti, G., Mele, G., 1993. Foreland deformational pattern in the Southern Adriatic Sea. *Annali di Geofisica* 36, 2, 229–247.
- Argnani, A., Frugoni, F., 1997. Foreland deformation in the Central Adriatic and its bearing on the evolution of the Northern Apennines. *Annals of Geophysics* 40, 771–780.
- Argnani, A., Gamberi, F., 1995. Stili strutturali al fronte della Catena Appenninica nell'Adriatico centro-settentrionale. *Studi Geologici Camerti* 1, 19–28.
- Argnani, A., Rovere, M., Bonazzi, C., 2009. Tectonics of the Mattinata fault, offshore south Gargano (southern Adriatic Sea, Italy): Implications for active deformation and seismotectonics in the foreland of the southern Apennines, *Geological Society of America Bulletin* 121, 9/10, 1421–1440, doi 10.1130/B26326.1.
- Atzori, S., Hunstad, I., Tolomei, C., Salvi, S., Ferretti, A., Cespa, S., 2007. Interseismic strain accumulation in the Gargano Promontory, central Italy. *Geophysical Research Abstracts* 9, Abstract EGU 2007-A-07651.
- Babbucci, D., Tamburelli, C., Viti, M., Mantovani, E., Albarello, D., D'Onza, F.; 2004: Relative motion of the Adriatic with respect to the confining plates: seismological and geodetic constraints. *Geophysical Journal International* 159, 765-775.

- Bajc, J., Aoudia, A., Saraò, A., Suhadolc, P., 2001. The 1998 Bovec–Krn mountain (Slovenia) earthquake sequence. *Geophysical Research Letters*, 28, 9, 1839–1842.
- Bally, A. W., Burbi, L., Cooper, C., Ghelardoni, R., 1986. Balanced sections and seismic reflection profiles across the central Apennines. *Memorie della Società Geologica Italiana* 35, 257–310.
- Baratta, M., 1894. Intorno ai fenomeni sismici avvenuti nella penisola Garganica durante il 1893, *Annali dell'Ufficio Centrale Meteorologico e Geodinamico Italiano* II 15, 1, 265–312.
- Barba, S., Carafa, M. M. C., Boschi, E., 2008. Experimental evidence for mantle drag in the Mediterranean, *Geophysical Research Letters* 35, L06302, doi: 10.1029/2008GL033281.
- Barchi, M., 2010. The Neogene-Quaternary evolution of the Northern Apennines: crustal structure, style of deformation and seismicity. *Journal of the Virtual Explorer* 36, Paper 11.
- Barchi, M., De Feyter, A., Magnani, M.B., Minelli, G., Piali, G., Sotera, B.M., 1998a. The structural style of the Umbria-Marche fold and thrust belt. *Memorie della Società Geologica Italiana* 52, 557–578.
- Barchi, M., Minelli, G., Piali, G., 1998b. The CROP 03 profile: a synthesis of results on deep structures of the Northern Apennines. *Memorie della Società Geologica Italiana* 52, 383–400.
- Basili, R., Barba, S., 2007. Migration and shortening rates in the northern Apennines, Italy: implications for seismic hazard. *Terra Nova* 19, 462–468, doi: 10.1111/j.1365-3121.2007.00772.x.
- Basili R., Burrato, P., Mariano, S., Mirabella, F., Ravaglia, A., Valensise, G., Vannoli, P., 2007. Identificazione e caratterizzazione delle sorgenti sismogenetiche, in: *Scenari di pericolosità sismica della fascia costiera marchigiana. La microzonazione sismica di Senigallia*. Mucciarelli, M., Tiberi, P. (Eds.), Regione Marche and INGV, 316 pp.
- Basili, R., Garcia Moreno, D., Kastelic, V., Nemser, E., Petricca, P., Sboras, S., Valensise, G., 2010. Developing seismogenic source models based on geologic fault data in the Euro-Mediterranean area: SHARE mission accomplished? *Proceedings of the 32nd General Assembly of European Seismological Commission*, Montpellier, 6–10 September 2010.
- Basili, R., Kastelic, V., Valensise, G., DISS Working Group 2009, 2009. DISS3 tutorial series: Guidelines for compiling records of the Database of Individual Seismogenic Sources, version 3, *Rapporti Tecnici INGV* 108, <http://portale.ingv.it/produzione-scientifica/rapporti-tecnici-ingv/archivio/rapporti-tecnici-2009/>.
- Basili, R., Valensise, G., Vannoli, P., Burrato, P., Fracassi, U., Mariano, S., Tiberti, M. M., Boschi, E., 2008. The Database of Individual Seismogenic Sources (DISS), version 3: Summarizing 20 years of research on Italy's earthquake geology. *Tectonophysics* 453, 20–43, doi: 10.1016/j.tecto.2007.04.014.
- Battaglia M., Murray M.H., Serpelloni E., and R. Bürgmann, 2004. The Adriatic region: an independent microplate within the Africa-Eurasia collision zone. *Geophysical Research Letters*, 31(9), L09605, doi: 10.1029/2004GL019723.

Benac, C., Juracic, M., Bakran-Petricioli, T., 2004. Submerged tidal notches in the Rijeka Bay NE Adriatic Sea: indicators of relative sea-level change and of recent tectonic movements. *Marine Geology* 212, 21–33, doi: 10.1016/j.margeo.2004.09.002.

Benac, C., Juracic, M., Blašković, I., 2008. Tidal notches in Vinodol Channel and Bakar Bay, NE Adriatic Sea: Indicators of recent tectonics. *Marine Geology* 248, 151–160, doi: 10.1016/j.margeo.2007.10.010.

Benetatos, C., Kiratzi, A., 2006. Finite-fault slip models for the 15 April 1979 (Mw 7.1) Montenegro earthquake and its strongest aftershock of 24 May 1979 (Mw 6.2). *Tectonophysics* 421, 129–143, doi: 10.1016/j.tecto.2006.04.009.

Bennett, R. A., Hreinsdóttir, S. n., Buble, G., Bašić, T., Bacić, Ž., Marjanović, M., Casale, G., Gendaszek, A., Cowan, D., 2008. Eocene to present subduction of southern Adria mantle lithosphere beneath the Dinarides. *Geology* 36, 3–6, doi: 10.1130/g24136a.1.

Bertotti, G., Casolari, E., Picotti, V., 1999. The Gargano Promontory, a contractional belt in the Adriatic plate. *Terra Nova* 11, 168–173.

Bigi, G., Cosentino, D., Parotto, M., Sartori, R., Scandone, P., 1983. Structural model of Italy. Scala 1:500.000. C.N.R., Progetto Finalizzato Geodinamica, Sottoprogetto: Modello strutturale tridimensionale.

Billi, A., 2003, Solution slip and separations on strike-slip fault zones: theory and application to the Mattinata Fault, Italy. *Journal of Structural Geology* 25, 703–715.

Billi, A., Gambini, R., Nicolai, C., Storti, F., 2007. Neogene–Quaternary intraforeland transpression along a Mesozoic platform-basin margin: the Gargano fault system, Adria, Italy. *Geosphere* 3, 1, 1–15.

Blašković, I., 1999. Tectonics of part of the Vinodol Valley within the model of the continental crust subduction. *Geologia Croatica* 52, 153-189.

Boccaletti, M., Calamita, F., Viandante, M. G., 2005. La Neo-Catena litosferica appenninica nata a partire dal Pliocene inferiore come espressione della convergenza Africa-Europa. *Bollettino della Società geologica italiana* 124, 87–105.

Boccaletti, M., Coli, M., Napoleone, G., 1977. Nuovi allineamenti strutturali da immagini Landsat e rapporti con l'attività sismica negli Appennini. *Bollettino della Società Geologica Italiana* 96, 679–694.

Boncio, P., Brozzetti, F., Lavecchia, G., 2000. Architecture and seismotectonics of a regional low-angle normal fault zone in Central Italy. *Tectonics* 19, 1038-1055.

Boschi, E., Ferrari, G., Gasperini, P., Guidoboni, E., Smriglio, G., Valensise, G., 1995. Catalogo dei Forti Terremoti in Italia dal 461 a.C. al 1980, ING Roma - SGA Bologna, con database su CD-ROM.

Brozzetti F., D'Amato D., Pace B., 2006. Complessità delle deformazioni neogeniche nell'avampese adriatico: nuovi dati strutturali dalle Isole Tremiti. *Rendiconti della Società Geologica Italiana (Nuova serie)* 2, 94–97.

Brückl, E., Bleibinhaus, F., Gosar, A., Grad, M., Guterch, A., Hrubcovà, P., Keller, G. R., Majdanski, M., Šumanovac, F., Tiira, T., Yliniemi, J., Hegedűs, E., Thybo, 2007, Crustal structure due to collisional and escape tectonics in the Eastern Alps region based on profiles Alp01 and Alp02 from the ALP 2002 seismic experiment, *Journal of Geophysical Research* 112, B06308, doi: 10.1029/2006JB004687.

Burrato, P., Ciucci, F., Valensise, G., 2003. An inventory of river anomalies in the Po Plain, Northern Italy: evidence for active blind thrust faulting. *Annals of Geophysics* 46, 5, 865-882.

Burrato, P., Poli, M.E., Vannoli, P., Zanferrari, A., Basili, R., Galadini, F., 2008. Sources of Mw 5+ earthquakes in northeastern Italy and western Slovenia: an updated view based on geological and seismological evidence. *Tectonophysics* 453, 157–176, doi: 10.1016/j.tecto.2007.07.009.

Buseti, M., Volpi, V., Barison, E., Giustiniani, M., Marchi, M., Ramella, R., Wardell, N., Zanolla, C., 2008. Meso-Cenozoic seismic stratigraphy and tectonic setting of the Gulf of Trieste (northern Adriatic). *GeoActa*, Special Publication 3, 15–28.

Buseti, M., Volpi, V., Nicolich, R., Barison, E., Romeo, R., Baradello, L., Brancatelli, G., Giustiniani, M., Marchi, M., Zanolla, C., Wardell, N., Nieto, D., Ramella, R., 2010. Dinaric tectonic features in the Gulf of Trieste (northern Adriatic Sea). *Bollettino di Geofisica Teorica ed Applicata* 51, 2–3, 117–128.

Butler, R. W. H., Mazzoli, S., Corrado, S., De Donatis, M., Di Bucci, D., Gambini, R., Naso, G., Nicolai, C., Scrocca, D., Shiner, P., Zucconi, V., 2004. Applying thick-skinned tectonic models to the Apennines thrust belt of Italy - Limitations and implications, in: McClay, K. R. (Ed.), *Thrust tectonics and hydrocarbon systems*. American Association of Petroleum Geologists Memoir 82, 647–667.

Calamita, F., Cello, G., Centamore, E., Deiana, G., Micarelli, A., Paltrinieri, W., Ridolfi, M., 1991. Stile deformativo e cronologia della deformazione lungo tre sezioni bilanciate dall'Appennino umbro-marchigiano alla costa adriatica. *Studi Geologici Camerti*, Vol. speciale 1, 295–314.

Calamita, F., Cello, G., Deiana, G., Paltrinieri, W., 1994. Structural styles, chronology rates of deformation, and time-space relationships in the Umbria-Marche thrust system (central Apennines, Italy). *Tectonics* 13, 873–881, doi:10.1029/94TC00276.

Calamita F., Satolli, S., Scisciani, V., Eserime, P., Pace, P., 2011. Contrasting styles of fault reactivation in curved orogenic belts: Examples from the Central Apennines (Italy). *Geological Society of America Bulletin* 123, 1097–1111 doi: 10.1130/B30276.1

Calderoni, G., Di Giovambattista, R., Burrato, P., Ventura, G., 2009. A seismic sequence from Northern Apennines (Italy) provides new insight on the role of fluids in the active tectonics of accretionary wedges. *Earth and Planetary Science Letters* 281, 99–109, doi: 10.1016/j.epsl.2009.02.015.

Calderoni, G., Di Giovambattista, R., Vannoli, P., Pucillo, S., Rovelli, A., 2012. Fault-trapped waves depict continuity of the fault system responsible for the 6 April 2009 Mw 6.3 L'Aquila earthquake, central Italy. *Earth and Planetary Science Letters* 323–324, 1–8, doi: 10.1016/j.epsl.2012.01.003.

Camassi, R., Bernardini, F., Castelli, V., Meletti, C., 2008. A 17th century destructive seismic crisis in the Gargano area: Its implications on the understanding of local seismicity, *Journal of Earthquake Engineering* 12, 8, 1223–1245, doi: 10.1080/13632460802212774.

Camassi, R., Caracciolo, C., Castelli, V. and Slejko, D., 2011. The 1511 Eastern Alps earthquakes: a critical update and comparison of existing macroseismic datasets. *Journal of Seismology* 15, 2, 191–213, doi: 10.1007/s10950-010-9220-9.

Canavari, M. 1885. Osservazioni intorno all'esistenza di una terraferma nell'attuale bacino adriatico. *Atti della Società Toscana di Scienze Naturali, Pisa, Proc. Verb.*, 4, 151–157.

Caporali, A., Aichhorn, C., Barlik, M., Becker, M., Fejes, I., Gerhatova, L., Ghitau, D., Grenerczy, G., Hefty, J., Krauss, S., et al., 2009. Surface kinematics in the Alpine-Carpathian-Dinaric and Balkan region inferred from a new multi-network GPS combination solution. *Tectonophysics* 474, 295–321, doi: 10.1016/j.tecto.2009.04.035.

Caputo, R., Poli, M.E., Zanferrari, A., 2010. Neogene-Quaternary tectonic stratigraphy of the eastern Southern Alps, NE Italy. *Journal of Structural Geology* 32, 1009–1027, doi: 10.1016/j.jsg.2010.06.004.

Carafa, M. M. C., Barba, S., 2011. Determining rheology from deformation data: The case of central Italy. *Tectonics* 30, TC2003, doi: 10.1029/2010TC002680.

Carminati, E., Doglioni, C., Barba, S., 2004. Reverse migration of seismicity on thrusts and normal faults. *Earth Sciences Reviews* 65, 195–222.

Castellarin, A., Cantelli, L., 2000. Neo-Alpine evolution of the Southern Eastern Alps. *Journal of Geodynamics* 30, 251–274, doi: 10.1016/S0264-3707(99)00036-8.

Castello, B., Selvaggi, G., Chiarabba, C., Amato, A., 2006. CSI Catalogo della sismicità italiana 1981-2002, versione 1.1, INGV-CNT, Roma, <http://csi.rm.ingv.it/>.

Catalano, R., Doglioni, C., Merlini, S., 2001. On the Mesozoic Ionian Basin. *Geophysical Journal International* 144, 49–64.

Channell, J. E. T., D'Argenio, B., Horvath, F., 1979. Adria, the African promontory, in *Mesozoic Mediterranean paleogeography*. *Earth-Science Reviews* 15, 213–292, doi 10.1016/0012-8252(79)90083-7.

Chiarabba, C., Jovane, L., Di Stefano, R., 2005. A new view of Italian seismicity using 20 years of instrumental recordings. *Tectonophysics* 395, 251–268, doi: 10.1016/j.tecto.2004.09.013.

Ciotoli, G., Lombardi, S., Morandi, S., Zarlenga, F., 2004. A multidisciplinary, statistical approach to study the relationships between helium leakage and neotectonic activity in a gas province: The Vasto basin, Abruzzo-Molise (central Italy). *American Association of Petroleum Geologists Bulletin* 88, 3, 355–372.

Ciotoli, G., Lombardi, S., Zarlenga, F., 2006. Natural leakage of helium from Italian sedimentary basins of the Adriatic structural margin, in: Lombardi, S., Altunina, L.K., Beaubien, S.E., (Eds.), *Advances in the Geological Storage of Carbon Dioxide*, *Nato Earth Science Series* 191–202, doi: 10.1007/1-4020-4471-2_16.

Colantoni, P., Tramontana, M., Tedeschi, R., 1990. Contributo alla conoscenza dell'avampaese apulo: struttura del Golfo di Manfredonia (Adriatico meridionale). *Giornale di Geologia Serie 3a* 52, 1–2, 19–32.

Console, R., Di Giovambattista, R., Favali, P., Presgrave, B. W., Smriglio, G., 1993. Seismicity of the Adriatic microplate. *Tectonophysics* 218, 343–354.

Coward, M. P., De Donatis, M., Mazzoli, S., Paltrinieri, W., Wezel, F.-C., 1999. Frontal part of the northern Apennines fold and thrust belt in the Romagna-Marche area (Italy): Shallow and deep structural styles. *Tectonics* 18, 559–574, doi: 10.1029/1999TC900003.

Cuffaro, M., Riguzzi, F., Scrocca, D., Antonioli, F., Carminati, E., Livani, M., Doglioni, C., 2010. On the geodynamics of the northern Adriatic plate, *Rendiconti dei Lincei-Scienze fisiche e naturali* 21, Suppl. 1, 253-279, doi: 10.1007/s12210-010-0098-9.

Cvijanović, D., 1981. Seizmicnost područja SR Hrvatske. Disertacija, Sveuciliste u Zagrebu, PMF, Zagreb.

D'Agostino, N., Avallone, A., Cheloni, D., D'Anastasio, E., Mantenuto, S., Selvaggi, G., 2008. Active tectonics of the Adriatic region from GPS and earthquake slip vectors. *Journal of Geophysical Research* 113, B12413, doi:10.1029/2008JB005860.

D'Agostino, N., Mantenuto, S., D'Anastasio, E., Giuliani, R., Mattone, M., Calcaterra, S., Gambino, P., Bonci, L., 2011. Evidence for localized active extension in the central Apennines (Italy) from global positioning system observations. *Geology* 39, 291–294, 10.1130/g31796.1.

de Alteriis, G., 1995. Different foreland basins in Italy: examples from the central and southern Adriatic Sea. *Tectonophysics* 252, 349–373.

de Alteriis, G., Aiello, G., 1993. Stratigraphy and tectonics offshore of Puglia (Italy, Southern Adriatic Sea). *Marine Geology* 113, 233–253.

De' Dominicis, A., Mazzoldi, G., 1987. Interpretazione geologico-strutturale del margine orientale della Piattaforma apula. *Memorie della Società Geologica Italiana* 38, 163–176.

De Martini, P. M., Burrato, P., Pantosti, D., Maramai, A., Graziani, L., Abramson, H., 2003. Identification of tsunami deposits and liquefaction features in the Gargano area (Italy): Paleoseismological implication, *Annals of Geophysics* 46, 5, 883–902.

Del Ben, A., Geletti, R., Mocnik, A., 2010. Relation between recent tectonics and inherited Mesozoic structures of the central-southern Adria plate. *Bollettino di Geofisica Teorica e Applicata* 52, 99–115.

Del Gaudio, V., Festa, V., Ripa, R.R., Iurilli, V., Pierri, P., Calcagnile, G., Moretti, M., Pieri P., Tropeano M., 2001. Evidence of Apulian crustal structures related to low energy seismicity (Murge - southern Italy). *Annali di Geofisica* 44, 1049-1066.

Del Gaudio, V., Pierri, P., Calcagnile G., Venisti N., 2005. Characteristics of the low energy seismicity of central Apulia (Southern Italy) and hazard implications. *Journal of Seismology* 9, 39-59.

Del Gaudio, V., Pierri, P., Frepoli, A., Calcagnile, G., Venisti, N., Cimini G., 2007. A critical revision of the seismicity of Northern Apulia (Adriatic Microplate - Southern Italy) and implications for the identification of seismogenic structures. *Tectonophysics* 436, 9-35, doi: 10.1016/j.tecto.2007.02.013.

Dercourt, J., Zonenshain, L.P., Ricou, L.E., Kazmin, V.G., Le Pichon, X., Knipper, A.L., Grandjacquet, C., Sbertshikov, I.M., Geyssant, J., Lepvirer, C., Pechersky, D.H., Boulin, J., Sibuet, J.C., Savostin, L.A., Sorokhtin, O., Westphal, M., Bazchenov, M.L., Lauer, J.P., Biju-Duval, B., 1986. Geological evolution of the Tethys belt from Atlantic to the Pamirs since the Lias, in: Aubouin, J., Le Pichon, X., Monin, A.S. (Eds.), *Evolution of the Tethys*. *Tectonophysics* 123, 241–315.

Devoti, R., Esposito, A., Pietrantonio, G., Pisani, A.R., Riguzzi, F., 2011. Evidence of large scale deformation patterns from GPS data in the Italian subduction boundary. *Earth and Planetary Science Letters* 311, 3–4, 230–241, doi: 10.1016/j.epsl.2011.09.034.

Devoti, R., Riguzzi, F., Cuffaro, M., Doglioni, C., 2008. New GPS constraints on the kinematics of the Apennines subduction. *Earth and Planetary Science Letters* 273, 163–174, doi: 10.1016/j.epsl.2008.06.031.

Dewey, J.F., Pitman, W.C., Ryan, W.B.F., Bonnin, J., 1973. Plate tectonic and the evolution of the Alpine system. *Geological Society of America Bulletin* 84, 3137–3180.

Di Bucci, D., Burrato, P., Vannoli, P., Valensise, G., 2010. Tectonic evidence for the ongoing Africa-Eurasia convergence in central Mediterranean foreland areas: A journey among long-lived shear zones, large earthquakes, and elusive fault motions. *Journal of Geophysical Research* 115, B12404, doi: 10.1029/2009JB006480.

Di Bucci, D., Mazzoli, S., 2002. Active tectonics of the Northern Apennines and Adria geodynamics: new data and a discussion. *Journal of Geodynamics* 34, 687–707.

Di Bucci, D., Mazzoli, S., 2003. The October-November 2002 Molise seismic sequence (southern Italy): an expression of Adria intraplate deformation. *Journal of the Geological Society* 160, 503–506.

Di Bucci, D., Ravaglia, A., Seno, S., Toscani, G., Fracassi, U., Valensise, G., 2006. Seismotectonics of the Southern Apennines and Adriatic foreland: insights on active regional E–W shear zones from analogue modeling. *Tectonics* 25, TC4015. doi: 10.1029/2005TC001898.

Di Bucci, D., Ridente, D., Fracassi, U., Trincardi, F., Valensise, G., 2009. Marine paleoseismology from very high resolution seismic imaging: The Gondola fault zone (Adriatic foreland). *Terra Nova* 21, 5, 393–400, doi: 10.1111/j.1365-3121.2009.00895.x.

Di Luccio, F., Fukuyama, E., Pino, N.A., 2005. The 2002 Molise earthquake sequence: What can we learn about the tectonics of southern Italy? *Tectonophysics* 405, 141–154.

DISS Working Group (2010). Database of Individual Seismogenic Sources (DISS), Version 3.1.1: A compilation of potential sources for earthquakes larger than M 5.5 in Italy and surrounding areas. <http://diss.rm.ingv.it/diss/>, © INGV 2010 - Istituto Nazionale di Geofisica e Vulcanologia.

- Doglioni, C., Bosellini, A., 1987. Eoalpine and mesoalpine tectonics in the Southern Alps. *Geologische Rundschau* 76, 735–754.
- Doglioni, C., Harabaglia, P., Merlini, S., Mongelli, F., Peccerillo, A., Piromallo, C., 1999. Orogens and slabs vs. their direction of subduction. *Earth-Science Reviews* 45, 167–208, doi: 10.1016/S0012-8252(98)00045-2.
- Doglioni, C., Mongelli, F., Pieri, P., 1994. The Puglia uplift (SE Italy): an anomaly in the foreland of the Apenninic subduction due to buckling of a thick continental lithosphere. *Tectonics* 13, 1309–1321.
- Drobne, K., Pavlovec, R., 1991. Paleocene and Eocene beds in Slovenia and Istria, in: Introduction to Paleogene SW Slovenia and Istria. Field-trip Guidebook IGCP Project 286, Early Paleogene Benthos, II meeting, Postojna, 19-27.
- Faccenna, C., Jolivet, L., Piromallo, C., Morelli, A., 2003. Subduction and the depth of convection in the Mediterranean mantle, *Journal of Geophysical Research* 108, doi: 10.1029/2001JB001690.
- Fantoni, R., Franciosi, R., 2010. Tectono-sedimentary setting of the Po Plain and Adriatic foreland. *Rendiconti Fisici Accademia dei Lincei* 21, 1, S197–S209, doi: 10.1007/s12210-010-0102-4.
- Favali, P., Funicello, R., Mattiotti, G., Mele, G., Salvini, F., 1993. An active margin across the Adriatic Sea central Mediterranean Sea). *Tectonophysics* 219, 109–117.
- Finetti, I., 1982. Structure, stratigraphy and evolution of central Mediterranean. *Bollettino di Geofisica Teorica e Applicata* 24, 247–312.
- Finetti, I., 1984, Struttura ed evoluzione della microplacca Adriatica, *Bollettino di Oceanografia Teorica ed Applicata* II 2, 115–123.
- Finetti, I. R., Boccaletti, M., Bonini, M., Del Ben, A., Geletti, R., Pipan, M., Sani, F., 2001. Crustal section based on CROP seismic data across the North Tyrrhenian-Northern Apennines-Adriatic Sea. *Tectonophysics* 343, 135–163, doi: 10.1016/S0040-1951(01)00141-X.
- Finetti, I., Bricchi, G., Del Ben, A., Pipan, M., Xuan, Z., 1987. Geophysical study of the Adria plate. *Memorie della Società Geologica Italiana* 40, 335–344.
- Finetti, I.R., Del Ben, A., 2005. Crustal tectono-stratigraphic setting of the Adriatic Sea from new CROP seismic data, in: Finetti, I.R. (Ed.), *Crop Project. Deep seismic exploration of the Central Mediterranean and Italy. Atlases in Geoscience* 1, Elsevier B.V., The Netherlands, 519–547.
- Fitzko, F., Suhadolc, P., Audia, A., Panza, G.F., 2005. Constrains on the location and mechanism of the 1511 Western-Slovenia earthquake from active tectonics and modeling of macroseismic data. *Tectonophysics* 404, 77–90.
- Fracassi U., Burrato P., Basili R., Bencini R., Di Bucci, D., Valensise, G., 2004. Deep faulting vs. upper faults: is the Apulian platform deforming Southern Italy? *Proceedings of the 32nd International Geological Congress, 20-28 August 2004, Firenze, Italy.*

Fracassi, U., Di Bucci, D., Ridente, D., Trincardi, F., Valensise, G., 2012. Recasting Historical Earthquakes in Coastal Areas (Gargano Promontory, Italy): Insights From Marine Paleoseismology. *Bulletin of the Seismological Society of America* 102, 1, 1–17, doi: 10.1785/0120110001.

Fracassi, U., Valensise, G., 2007. Unveiling the sources of the catastrophic 1456 multiple earthquake: Hints to an unexplored tectonic mechanism in southern Italy. *Bulletin of the Seismological Society of America* 97, 3, 725–748, doi: 10.1785/0120050250.

Fracassi, U., Vannoli, P., Burrato, P., Basili, R., Tiberti, M.M., Di Bucci, D., Valensise, G., 2006. From Extension to Transcurrence: Regime Transition as a new key to Interpret Seismogenesis in the Southern Apennines (Italy). *Proceedings of the 2006 AGU Fall Meeting*, 11-15 December 2006, San Francisco, CA, USA.

Frepoli, A., Amato, A., 1997. Contemporaneous extension and compression in the Northern Apennines from earthquake fault-plane solutions. *Geophysical Journal International* 129, 368–388, doi: 10.1111/j.1365-246X.1997.tb01589.x.

Frepoli, A., Amato, A., 2000. Spatial variation in stresses in peninsular Italy and Sicily from background seismicity. *Tectonophysics* 317, 1–2, 109-124.

Galadini, F., Poli, M. E., Zanferrari, A., 2005. Seismogenic sources potentially responsible for earthquakes with $M \geq 6$ in the eastern Southern Alps (Thiene-Udine sector, NE Italy). *Geophysical Journal International* 161, 739–762, doi: 10.1111/j.1365-246X.2005.02571.x.

Gambini, R., and Tozzi, M., 1996. Tertiary geodynamic evolution of the Southern Adria microplate. *Terra Nova* 8, 593–602, doi: 10.1111/j.1365-3121.1996.tb00789.x.

Gasparini, C., Iannaccone, G., Scarpa, R., 1985. Fault-plane solutions and seismicity of the Italian peninsula. *Tectonophysics* 117, 59–78, doi: 10.1016/0040-1951(85)90236-7.

Geletti, R., Del Ben, A., Busetti, M., Ramella, R., Volpi, V., 2008. Gas seeps linked to salt structures in the Central Adriatic Sea. *Basin Research* 20, 473–487, doi: 10.1111/j.1365-2117.2008.00373.x.

Global CMT Catalog, Ekström, G., Nettles M. (Overseers), available at <http://www.globalcmt.org/> (last accessed 2 March 2012).

Grandić, S., Biancone, M., Samaržija, J., 2002. Geophysical and stratigraphic evidences of the Adriatic Triassic rift structures. *Memorie della Società Geologica Italiana* 57, 315–325.

Grandić, S., Boromisa-Balaš, E., Šušterčić, S., Kolbah, S., 1999. Hydrocarbon possibilities in the eastern Adriatic slope zone of Croatian offshore area. *Nafta* 50/2, 51–73.

Grandić, S., Kratkovic, I., Kolbah, S., 2007. Review of the hydrocarbon plays in the Croatian offshore and Periadriatic areas. *Nafta* 58, 146–158.

Grandić, S., Kratkovic, I., Kolbah, S., Samaržija, J., 2004. Hydrocarbon potential of stratigraphic and structural traps of the Ravni Kotari area Croatia. *Nafta* 55, 311–327.

Grandić, S., Markulin, Z., 2000. Triassic synrift euxinic basins as a factor of exploration risk in the Croatian offshore area, International Symposium of Petroleum Geology, 22-24 April 1999, Nafta Sp. Issue, 41–50.

Grenerczy, G., Sella, G., Stein, S., Kenyeres, A., 2005. Tectonic implications of the GPS velocity field in the northern Adriatic region. *Geophysical Research Letters* 32, L16311, doi: 10.1029/2005GL022947.

Gruppo di lavoro CPTI, 2004. Catalogo Parametrico dei Terremoti Italiani, versione 2004 (CPTI04), INGV, Bologna, <http://emidius.mi.ingv.it/CPTI04/>.

Guidoboni, E., Comastri, A., 2005. Catalogue of Earthquakes and Tsunamis in the Mediterranean Area from the 11th to the 15th Century, Istituto Nazionale di Geofisica e Vulcanologia–SGA, Bologna, Italy, 1037 pp.

Guidoboni, E., Ferrari, G., Mariotti, D., Comastri, A., Tarabusi, G., Valensise, G., 2007. CFTI4Med, Catalogue of Strong Earthquakes in Italy (461 B.C.-1997) and Mediterranean Area (760 B.C.-1500). INGV–SGA, <http://storing.ingv.it/cfti4med/>.

Hanks, T. C., Kanamori, H., 1979. A moment magnitude scale. *Journal of Geophysical Research* 84, 2348–2350.

Heidbach, O., Tingay, M., Barth, A., Teinecker, J., Kurfes, D., Müller, B., 2010. Global crustal stress pattern based on the World Stress Map database release 2008. *Tectonophysics* 462, doi: 10.1016/j.tecto.2009.1007.1023.

Herak, D., Herak, M., Prelogović, E., Markusić, S., Markulin, Z., 2005. Jabuka island (Central Adriatic Sea) earthquakes of 2003. *Tectonophysics* 398, 167–180, doi: 10.1016/j.tecto.2005.01.007.

Herak, M., Herak, D., Markušić, S., 1995. Fault plane solutions for earthquakes (1956–1995) in Croatia and neighbouring regions, *Geofizika* 12, 43–56.

Herrmann, R. B., Malagnini, L., Munafò, I., 2011. Regional Moment Tensors of the 2009 L'Aquila Earthquake Sequence. *Bulletin of the Seismological Society of America* 101, 975–993, doi: 10.1785/0120100184.

Hippolyte, J.C., Angelier, J., Roure, F., 1994. A major geodynamic change revealed by Quaternary stress patterns in the Southern Apennines (Italy). *Tectonophysics* 230, 199–210.

ISIDe Working Group (INGV, 2010), Italian Seismological Instrumental and parametric database: <http://iside.rm.ingv.it>.

Ivančić, I., Herak, D., Markušić, S., Sović, I., Herak, M., 2006. Seismicity of Croatia in the period 2002–2005. *Geofizika* 23, 87–103.

Juračić, M., Novosel, A., Tibljaš, D., Balen, D., 2004. Jabuka Shoal, a New Location with Igneous Rocks in the Adriatic Sea. *Geologica Croatica* 57, 1, 81–85.

Kastelic, V. and Carafa, M. M. C., 2012. Fault slip rates for the active External Dinarides thrust-and-fold belt. *Tectonics* 31, TC3019, doi: 10.1029/2011TC003022.

- Kastelic, V., Vrabec, M., Cunningham, D., Gosar, A., 2008. Neo-Alpine structural evolution and present-day tectonic activity of the eastern Southern Alps: the case of the Ravne Fault, NW Slovenia. *Journal of Structural Geology* 30, 963–975, doi: 10.1016/j.jsg.2008.03.009.
- Korbar, T., 2009. Orogenic evolution of the External Dinarides in the NE Adriatic region: a model constrained by tectonostratigraphy of Upper Cretaceous to Paleogene carbonates. *Earth-Science Reviews* 96, 296–312.
- Kuk, V., Prelogovic, E., Dragicevic, I., 2000. Seismotectonically active zones in the Dinarides. *Geologia Croatica* 53, 295–303.
- Latorre, D., Amato, A., Chiarabba, C., 2010. High resolution seismic imaging of the Mw 5.7, 2002 Molise, southern Italy, earthquake area: Evidence of deep fault reactivation. *Tectonics* 29, TC4014, doi: 10.1029/2009TC002595.
- Lavecchia, G., Boncio, P., Creati, N., 2003. A lithospheric-scale seismogenic thrust in central Italy. *Journal of Geodynamics* 36, 79–94, doi: 10.1016/S0264-3707(03)00040-1.
- Lippitsch, R., Kissling, E., Ansorge, J., 2003. Upper mantle structure beneath the Alpine orogen from high-resolution teleseismic tomography. *Journal of Geophysical Research* 108, doi: 10.1029/2002JB002016.
- Locati, M., Camassi, R., Stucchi, M., (Eds.), 2011. DBMI11, the 2011 version of the Italian Macroseismic Database. Milano, Bologna, <http://emidius.mi.ingv.it/DBMI11>.
- Lorito, S., Tiberti, M. M., Basili, R., Piatanesi, A., Valensise, G., 2008. Earthquake-generated tsunamis in the Mediterranean Sea: Scenarios of potential threats to Southern Italy. *Journal of Geophysical Research* 113, B01301, doi: 10.1029/2007JB004943.
- Lort, J. M., 1971. The tectonics of the eastern Mediterranean: A geophysical review, *Reviews of Geophysics* 9, 2, 189–216.
- Maesano, F.E., Toscani, G., Burrato, P., Mirabella, F., D'Ambrogi, C., Basili, R., this issue. Deriving thrust fault slip rates from 3D geological modeling: examples from the Marche coastal and offshore contraction belt, northern Apennines, Italy. Submitted to *Marine and Petroleum Geology*.
- Mantovani, E., Boschi, E., Albarello, D., Babbucci, D. & Mucciarelli, M., 1991. Regularities in time and space distribution of seismicity in the Periadriatic regions: tectonic implications, *Tectonophysics*, 188, 349–356.
- Maramai, A., Graziani, L., Tinti, S., 2007. Investigation on tsunami effects in the central Adriatic Sea during the last century—a contribution. *Natural Hazards and Earth System Sciences* 7, 15–19.
- Markušić, S., Herak, D., Ivančić, I., Sovic, I., Herak, M., Prelogovic, E., 1998. Seismicity of Croatia in the period 1993-1996 and the Ston-Slano earthquake of 1996. *Geofizika* 15, 83–101.
- Markušić, S., Some, J., Herak, D., 1990. Seismicity of Croatia and the surrounding areas in 1988. *Geofizika* 7, 121–134.
- McKenzie, D., 1972. Active tectonics of the Mediterranean region, *Geophysical Journal of the Royal Astronomical Society* 30, 109–185.

Malinverno, A., Ryan, W.B.F., 1986. Extension in the Tyrrhenian Sea and shortening in the Apennines as result of arc migration driven by sinking of the lithosphere. *Tectonics* 5, 2, 227–245.

Meletti, C., Galadini, F., Valensise, G., Stucchi, M., Basili, R., Barba, S., Vannucci, G., Boschi, E., 2008. A seismic source zone model for the seismic hazard assessment of the Italian territory. *Tectonophysics* 450, 85–108, doi: 10.1016/j.tecto.2008.01.003.

Milano, G., Di Giovambattista, R., Ventura, G., 2005. Seismic constraints on the present-day kinematics of the Gargano foreland, Italy, at the transition zone between the southern and northern Apennines belts, *Geophysical Research Letters* 32, L24308, doi: 10.1029/2005GL024604.

Montone, P., Mariucci, M. T., Pierdominici, S., 2012. The Italian present-day stress map. *Geophysical Journal International*, doi: 10.1111/j.1365-246X.2012.05391.x.

Morelli, D., 2002. Evoluzione tettonico-stratigrafica del Margine Adriatico compreso tra il Promontorio garganico e Brindisi. *Memorie della Società Geologica Italiana* 57, 343–353.

Nanni, T., Vivalda, P., 1987, Influenza della tettonica trasversale sulla morfogenesi delle pianure alluvionali marchigiane, *Geografia Fisica e Dinamica Quaternaria* 10, 180–192.

National Geophysical Data Center / World Data Center (NGDC/WDC) Global Historical Tsunami Database, Boulder, CO, USA, available at http://www.ngdc.noaa.gov/hazard/tsu_db.shtml, last accessed 2 March 2012.

Oldow, J. S., Ferranti, L., Lewis, D. S., Campbell, J. K., D'Argenio, B., Catalano, R., Pappone, G., Carmignani, L., Conti, P., Aiken, C. L. V., 2002. Active fragmentation of Adria, the north African promontory, central Mediterranean orogen. *Geology* 30, 779–782, doi: 10.1130/0091-7613(2002)030<0779:afoatn>2.0.co;2.

Papazachos, B. C., Comninakis, P. E., Scordilis, E. M., Karakaisis, G. F., Papazachos, C. B., 2009. A catalogue of earthquakes in Mediterranean and surrounding area for the period 1901-2008, University of Thessaloniki.

Pasarić, M., Brizuela, B., Graziani, L., Maramai, A., Orlić, M., 2012. Historical tsunamis in the Adriatic Sea. *Natural Hazards* 61, 281–316, doi: 10.1007/s11069-011-9916-3.

Paulatto, M., Pinat, T., Romanelli, F., 2007. Tsunami hazard scenarios in the Adriatic Sea domain, *Natural Hazards and Earth System Science* 7, 309–325.

Piccardi, L., 2005. Paleoseismic evidence of legendary earthquakes: the apparition of Archangel Michael at Monte Sant'Angelo (Italy). *Tectonophysics* 408, 113–128.

Piccardi, L., Sani, F., Moratti, G., Cunningham, D., Vittori, E., 2011. Present-day geodynamics of the circum-Adriatic region: An overview. *Journal of Geodynamics* 51, 81–89, doi: 10.1016/j.jog.2010.09.002.

Piromallo, C., Morelli, A., 2003. P wave tomography of the mantle under the Alpine-Mediterranean area. *Journal of Geophysical Research* 108, doi: 10.1029/2002JB001757.

Placer, L., 2007. Kraški rob. Geološki prerez vzdolz AC Kozina-Koper. Kraški rob (landscape term). Geological section along the motor way Kozina-Koper (Capodistria). *Geologija* 50, 29–44.

Placer, L., Košir, A., Popit, T., Šmuc, A., Juvan, G., 2004. The Buzet Thrust Fault in Istria and overturned carbonate mega-beds in the Eocene flysch of the Dragonia Valley (Slovenia). *Geologija* 47, 193–198.

Pleničar, M., Polšak, A., Šikić, D., 1969. Basic Geological Map of SFRJ, sheet Trieste, 1:100 000. Geological survey Belgrade.

Pondrelli, S., Salimbeni, S., Ekström, G., Morelli, A., Gasperini, P., Vannucci, G., 2006. The Italian CMT dataset from 1977 to the present. *Physics of the Earth and Planetary Interiors* 159, 286–303, doi: 10.1016/j.pepi.2006.07.008.

Pondrelli, S., Salimbeni, S., Morelli, A., Ekström, G., Postpischl, L., Vannucci, G., Boschi, E., 2011. European-Mediterranean Regional Centroid Moment Tensor catalog: Solutions for 2005–2008. *Physics of the Earth and Planetary Interiors* 185, 74–81, doi: 10.1016/j.pepi.2011.01.007.

Prelogović, E., Kuk, V., Buljan, R., 1998. The structural fabric and seismotectonic activity of northern Velebit: some new observations. *Rudarsko-geološki-naftni zbornik* 10, 39–42.

Prelogović, E., Pribicevic, B., Ivkovic, Z., Dragicevic, I., Buljan, R., Tomljenovic, B., 2003. Recent structural fabric of the Dinarides and tectonically active zones important for petroleum-geological exploration in Croatia. *Nafta* 55, 155–161.

Renner, G., Slejko, D., 1994. Some comments on the seismicity of the Adriatic region. *Bollettino di Geofisica Teorica e Applicata* 36, 381 - 398.

Ricci Lucchi, F., 1975. Miocene paleogeography and basin analysis in the Periadriatic Apennines, in: *Geology of Italy*. Petroleum Exploration Society of Libia, Tripoli, 129–236.

Ridente, D., Fracassi, U., Di Bucci, D., Trincardi, F., Valensise, G., 2008a. Middle Pleistocene to Holocene activity of the Gondola Fault Zone (Southern Adriatic Foreland): deformation of a regional shear zone and seismotectonic implications. *Tectonophysics* 453, 110–21, doi: 10.1016/j.tecto.2007.05.009.

Ridente, D., Trincardi, F., 2006. Active foreland deformation evidenced by shallow folds and faults affecting late Quaternary shelf-slope deposits (Adriatic Sea, Italy). *Basin Research* 18, 2, 171–188. doi: 10.1111/j.1365-2117.2006.00289.x.

Ridente, D., Trincardi, F., Piva, A., Asioli, A., Cattaneo, A., 2008b. Sedimentary response to climate and sea level changes during the past 400 ka from borehole PRAD1-2 (Adriatic Margin). *Geochemistry Geophysics Geosystems*, 9, Q09R04, doi: 10.1029/2007GC001783.

Riguzzi, F., Tertulliani, A., Gasparini, C., 1989. Study of the seismic sequence of Porto San Giorgio (Marche)–3 July 1987. *Il Nuovo Cimento C* 12, 453–466, doi: 10.1007/BF02525078.

Rovida, A., Camassi, R., Gasperini, P., Stucchi, M. (Eds.), 2011. CPTI11, the 2011 version of the Parametric Catalogue of Italian Earthquakes. Milano, Bologna, <http://emidius.mi.ingv.it/CPTI>.

Royden, L., Patacca, E., Scandone, P., 1987. Segmentation and configuration of subducted lithosphere in Italy: an important control on thrust-belt and foredeep-basin evolution. *Geology* 15, 714–717.

Santini, S., 2003. A note on Northern Marche seismicity: new focal mechanisms and seismological evidence. *Annals of Geophysics* 46, 725–731.

Scisciani, V., Calamita, F., 2009. Active intraplate deformation within Adria: Examples from the Adriatic region. *Tectonophysics* 476, 57–72, doi: 10.1016/j.tecto.2008.10.030.

Scisciani, V., Calamita, F., Tavarnelli, E., Rusciadelli, G., Ori, G.G., Paltrinieri, W., 2001. Foreland-dipping normal faults in the inner edges of syn-orogenic basins: a case from the Central Apennines, Italy. *Tectonophysics* 330, 211–224.

Scisciani, V., Tavarnelli, E., Calamita, F., 2002. The interaction of extensional and contractional deformations in the outer zones of the Central Apennines, Italy. *Journal of Structural Geology* 24, 1647–1658, doi: 10.1016/S0191-8141(01)00164-X.

Scrocca, D., 2006. Thrust front segmentation induced by differential slab retreat in the Apennines (Italy). *Terra Nova* 18, 154–161, doi: 10.1111/j.1365-3121.2006.00675.x.

Scrocca, D., Carminati, E., Doglioni, C., Marcantoni, D., Lacombe, O., Roure, F., Lavé, J., Vergés, J., 2007. Slab Retreat and Active Shortening along the Central-Northern Apennines Thrust Belts and Foreland Basins, in: *Thrust belts and foreland basins: from fold kinematics to hydrocarbon systems*, O. Lacombe, J. Lave', F. Roure and J. Verges (Editors). *Frontiers in Earth Sciences*, Springer, 471-487, doi: 10.1007/978-3-540-69426-7_25.

Scrocca, D., Doglioni, C., Innocenti, F., Manetti, P., Mazzotti, A., Bertelli, L., Burbi, L., D'Offizi, S., 2003. CROP Atlas – Seismic reflection profiles of the Italian crust. *Memorie Descrittive della Carta Geologica d'Italia* 62.

Servizio Geologico d'Italia, in press. Note illustrative della Carta Geologica d'Italia alla scala 1:50.000, Foglio 266, Mercato Saraceno. http://www.isprambiente.gov.it/MEDIA/carg/note_illustrative/266_Mercato_Saraceno.pdf, published by ISPRA.

Shebalin, N. V., Karnik, V., Hadzievski, D., 1974. *Balkan Region-Catalogue of Earthquakes*, UNESCO Office, Skopje.

Šikić, D., Plenicar, M., Šparica, M., 1972. *Basic Geological Map of SFRJ*, sheet Ilirska Bistrica, 1:100 000. Geological survey, Belgrade.

Slejko, D., Carulli, G.B., Garcia, J., Santulin, M., 2011. The contribution of “silent” faults to the seismic hazard of the northern Adriatic Sea. *Journal of Geodynamics* 51, 2–3, 166–178, doi: 10.1016/j.jog.2010.04.009.

Soloviev, S.L., Go, Ch.N., 1974. *A catalogue of tsunamis on the western shore of the Pacific Ocean*, Moscow, "Nauka" Publishing House, 308p. English translation: Soloviev S.L., Go Ch.N. (1984). *A catalogue of tsunamis on the western shore of the Pacific ocean*, Translation by Canada Institute for Scientific and Technical Information, National Research Council, Ottawa, Canada KIA OS2.

Soloviev, S. L., Solovieva, O. N., Go, C. N., Kim, K. S., Shchetnikov, N. A., 2000. *Tsunamis in the Mediterranean Sea, 2000 BC-2000 AD*, Kluwer Academic Publisher.

Suess, E., 1883. *Das Antlitz der Erde*. Tempsky, Prag, Freytag, Leipzig.

Šumanovac, F., Orešković, J., Grad, M., Group, A. L. P. W., 2009. Crustal structure at the contact of the Dinarides and Pannonian basin based on 2-D seismic and gravity interpretation of the Alp07 profile in the ALP 2002 experiment. *Geophysical Journal International* 179, 615–633, doi: 10.1111/j.1365-246X.2009.04288.x.

Tari, V., 2002. Evolution of the northern and western Dinarides: a tectonostratigraphic approach. *Stephan Mueller Special Publication Series* 1, 223–236.

Tari-Kovačić, V., 1998. Geodynamics of the Middle Adriatic offshore area, Croatia, based on stratigraphic and seismic analysis of Paleogene beds. *Acta Geologica Hungarica* 41, 313–326.

Tari-Kovačić, V., Kalac, K., Lučić, D., Benić, J., 1998. Stratigraphic analysis of Paleogene beds in some off-shore wells (Central Adriatic Area, Croatia), *Slovenska akademija znanosti in umetnosti*.

Tesauro, M., Kaban, M. K., Cloetingh, S. A. P. L., 2009. A new thermal and rheological model of the European lithosphere. *Tectonophysics* 476, 478–495.

Thessaloniki Macroseismic Database, 2010. Macroseismic Data of the University of Thessaloniki, compiled and made available to the public in the frame of the activities of the EU NERIES project, NA4 module "A Distributed Archive of Historical Earthquake Data", <http://www.emidius.eu/AUTH/>.

Tiberti, M. M., Lorito, S., Basili, R., Kastelic, V., Piatanesi, A., Valensise, G., 2008. Scenarios of earthquake-generated tsunamis for the Italian Coast of the Adriatic Sea, in *Tsunami Science Four Years After the 2004 Indian Ocean Tsunami, Part I: Modelling*, P. Cummins, L. Kong, and K. Satake (Editors), *Pure and Applied Geophysics Topical Volumes* 165, 11/12, 2117–2142, doi: 10.1007/s00024-008-0417-6.

Tinti, S., Maramai, A., Favali, P., 1995. The Gargano Promontory: An important seismogenic-tsunamigenic area, *Marine Geology* 122, 2, 227–241, doi: 10.1016/0025-3227(94)00096-4.

Tinti, S., Maramai, A., Graziani, L., 2004. The new catalogue of Italian tsunamis. *Natural Hazards* 33, 439–465.

Tondi, E., Piccardi, L., Cacon, S., Kontny, B., Cello, G., 2005. Structural and time constraints for dextral shear along the seismogenic Mattinata fault (Gargano, southern Italy). *Journal of Geodynamics* 40, 134–152, doi: 10.1016/j.jog.2005.07.003.

Tramontana, M., Morelli, D., Colantoni, P., 1995. Tettonica plio-quadernaria del sistema sud-garganico (settore orientale) nel quadro evolutivo dell'Adriatico centro-meridionale. *Studi Geologici Camerti Volume Speciale* 1995/2, 467–473.

Valensise, G., Pantosti, D. (Eds.), 2001, *Database of Potential Sources for Earthquakes Larger than M 5.5 in Italy*. *Annali di Geofisica* 44, Suppl. 1, with CD-ROM.

Valensise, G., Pantosti, D., Basili, R., 2004. Seismology and Tectonic Setting of the 2002 Molise, Italy, Earthquake. *Earthquake Spectra* 20, S1, 23–37.

Vannoli, P., Basili, R., Valensise, G., 2004. New geomorphic evidence for anticlinal growth driven by blind-thrust faulting along the northern Marche coastal belt (central Italy). *Journal of Seismology* 8, 297–312.

Vannoli, P., Burrato, P., Fracassi, U., Valensise, G., 2012. A fresh look at the seismotectonics of the Abruzzi (Central Apennines) following the 6 April 2009 L'Aquila earthquake (Mw 6.3). *Bollettino della Società Geologica Italiana (Italian Journal of Geosciences)*, in press.

Venisti, N., Calcagnile, G., Del Gaudio, V. and Pierri, P., 2004. Combined analysis of seismic and gravimetric data in the Adriatic plate. *Physics of the Earth and Planetary Interiors* 142, 89-100

ViDEPI, 2010. Visibilità dei dati afferenti all'attività di esplorazione petrolifera in Italia. © 2009-2010 Progetto ViDEPI - Ministero dello Sviluppo Economico UNMIG - Società Geologica Italiana - Assomineraria, <http://www.videpi.com>.

Viti M., D'Onza, F., Mantovani, E., Albarello, D., Cenni, N., 2003. Post-seismic relaxation and earthquake triggering in the southern Adriatic region. *Geophysical Journal International* 153, 645-657.

Wegmann, K.W., Pazzaglia, F.J., 2009. Late Quaternary fluvial terraces of the Romagna and Marche Apennines, Italy: Climatic, lithologic, and tectonic controls on terrace genesis in an active orogen. *Quaternary Science Reviews* 28, 137-165, doi: 10.1016/j.quascirev.2008.10.006.

Wells, D. L., Coppersmith, K. J., 1994. New empirical relationships among magnitude, rupture length, rupture width, rupture area, and surface displacement. *Bulletin of the Seismological Society of America* 84, 974–1002.

Westaway, R., 1990. Present-day kinematics of the plate boundary zone between Africa and Europe, from Azores to the Aegean. *Earth and Planetary Science Letters* 96, 393–406.

Wortel, M. J. R., Spakman, W., 2000. Subduction and Slab Detachment in the Mediterranean-Carpathian Region. *Science* 290, 1910–1917, doi: 10.1126/science.290.5498.1910.

Wortmann, U.G., Weissert, H., Funk, H., Hauck, J., 2001. Alpine plate kinematics revisited: the Adria problem. *Tectonics* 20, 134–147.

Zonno, G., Basili, R., Meroni, F., Musacchio, G., Mai P. M., Valensise, G., 2012. High-frequency maximum observable shaking map of Italy from fault sources. *Bull. Earthquake Eng.* 4, 1,075-1,107, DOI 10.1007/s10518-012-9346-y.

FIGURE CAPTIONS

Figure 1:

Key structural, seismicity and geodynamic characteristics of the broader Adriatic domain. a) in blue, polygons encircling the five regions of the Adriatic domain discussed in this paper (with acronyms); black polylines indicate location of profiles shown in Figure 2, with corresponding numbers (taken after Fantoni and Franciosi, 2010). Official Code for the country names: IT = Italy, SI = Slovenia, HR = Croatia, BA = Bosnia and Herzegovina, ME = Montenegro; b) main structural elements of the Adriatic domain. Data taken from: Bigi et al., 1983 and Ivančić et al. (2006). Regional shear zones (from north to south): AVM = Arbia-Val Marecchia Line, OAS = Olevano-Antrodoco-Sibillini Line, OR = Ortona-Roccamonfina Line, NA = Northern Abruzzo shear zone, TL = Tremiti Line, MG = Molise-Gondola shear zone; c) earthquake epicentral locations from various catalogs; location of recorded tsunami effects taken from Pasarić et al. (2012) and from NOAA-NGDC catalog; focal mechanism solutions from Pondrelli et al. (2006); d) blue arrows are horizontal velocity vectors (Devoti et al., 2011); red lines indicate the orientation of the maximum compressive stress (Heidbach et al., 2010).

Figure 2:

Three regional cross-sections redrawn from the profiles 5, 6 and 7 of Fantoni and Franciosi (2010), showing the geometry of the Northern and Central Apennines and External Dinarides thrust belts. Faults included in the DISS database as CSS are highlighted in red and labeled with their ID. The ITCS027 source is not included in the sources of the Adriatic domain and is here highlighted in grey. All these sources are mapped in figures 3-8. Question marks emphasize those sources whose geometry do not fit that proposed by Fantoni and Franciosi (2010) but follow other interpretations. Further insights on these sources are discussed in the text.

Figure 3:

Characteristics of the North-Eastern Adriatic (AD1) region.

Summary table of main characteristics.

The list of $M \geq 5.5$ and/or $I_0 \geq 8$ historical and instrumental earthquakes associated with the seismogenic sources of AD1. Catalogue code: 1 = Rovida et al., 2011.

The list of earthquake-generated tsunamis of AD1. Name of the localities affected cells refer to localities reporting the particular event. Intensity scales: SA = Sieberg-Ambraseys (Ambraseys, 1962); SG = Soloviev and Go (Soloviev and Go, 1974). Catalogue code: 1 = Pasarić et al., 2012; 2 = NOAA/WDC Tsunami Event Database.

Map of the seismogenic sources in the Adriatic domain. ISS of the Adriatic domain are shown as blue rectangulars, CSS as orange polygons with a orange polylines. Sources not included in this study, but present in DISS and SHARE databases, are shown in grey polygons and polylines (CSSs) and grey rectangulars (ISSs).

Map of the seismogenic sources in AD1. The CSS belonging to the AD1 are shown as labeled polygons with a red polyline. The ISS belonging to the AD1 are shown as labeled blue rectangulars.

The list of ISSs of AD1 with their parameters.

The list of CSSs of AD1 with their parameters.

Figure 4:

Characteristics of the Eastern Adriatic (AD2) region.

Summary table of main characteristics. The list of $M \geq 5.5$ and/or $I_0 \geq 8$ historical and instrumental earthquakes associated with the seismogenic sources of AD2. Catalogue code: 1 = Rovida et al., 2011; 3 = Herak et al., 1995; 4 = Papazachos et al., 2009; 5 = Shebalin, 1974; 6 = Markušić et al., 1998; 7 = Herak et al., 2005; 8 = Thessaloniki Macroseismic earthquake catalogue, 2010.

The list of earthquake-generated tsunamis of AD2. Name of the localities affected cells refer to localities reporting the particular event. Intensity scales; SA = Sieberg-Ambraseys (Ambraseys, 1962); SG = Soloviev and Go (Soloviev and Go, 1974). Catalogue code: 1 = Pasarić et al., 2012; 2 = NOAA/WDC Tsunami Event Database.

Map of the seismogenic sources in AD2. The CSS belonging to the AD2 are shown as labeled polygons with a red polyline. The ISS belonging to the AD2 are shown as labeled blue rectangles. For a general map of all Adriatic domain seismogenic sources see Figure 3.

The list of ISSs of AD2 with their parameters.

The list of CSSs of AD2 with their parameters.

Figure 5:

Characteristics of the Central Adriatic (AD3) region.

Summary table of main characteristics.

The list of $M \geq 5.5$ and/or $I_o \geq 8$ historical and instrumental earthquakes associated with the seismogenic sources of AD3. Catalogue code: 1 = Rovida et al., 2011; 7 = Herak et al., 2005.

The list of earthquake-generated tsunami of AD3. Name of the localities affected cells refer to localities reporting the particular event. Intensity scales; SA = Sieberg-Ambraseys (Ambraseys, 1962); SG = Soloviev and Go (Soloviev and Go, 1974). Catalogue code: 1 = Pasarić et al., 2012; 2 = NOAA/WDC Tsunami Event Database.

Map of the seismogenic sources in AD3. The CSS belonging to the AD3 are shown as labeled polygons with a red polyline. The ISS belonging to the AD3 are shown as labeled blue rectangles. For a general map of all Adriatic domain seismogenic sources see Figure 3.

The list of ISSs of AD3 with their parameters.

The list of CSSs of AD3 with their parameters.

Figure 6:

Characteristics of the Southern Western Adriatic (AD4) region.

Summary table of main characteristics.

The list of $M \geq 5.5$ and/or $I_o \geq 8$ historical and instrumental earthquakes associated with the seismogenic sources of AD4. Catalogue code: 1 = Rovida et al., 2011; 2 = Locati et al., 2011.

The list of earthquake-generated tsunami of AD4. Name of the localities affected cells refer to localities reporting the particular event. Intensity scales; SA = Sieberg-Ambraseys (Ambraseys, 1962); SG = Soloviev and Go (Soloviev and Go, 1974). Catalogue code: 1 = Pasarić et al., 2012; 2 = NOAA/WDC Tsunami Event Database.

Map of the seismogenic sources in AD4. The CSS belonging to the AD4 are shown as labeled polygons with a red polyline. The ISS belonging to the AD4 are shown as labeled blue rectangles. For a general map of all Adriatic domain seismogenic sources see Figure 3.

The list of ISSs of AD4 with their parameters.

The list of CSSs of AD4 with their parameters.

Figure 7:

Characteristics of the Central Western Adriatic (AD5) region.

Summary table of main characteristics.

The list of $M \geq 5.5$ and/or $I_o \geq 8$ historical and instrumental earthquakes associated with the seismogenic sources of AD5. Catalogue code: 1 = Rovida et al., 2011.

The list of earthquake-generated tsunami of AD5. Name of the localities affected cells refer to localities reporting the particular event. Intensity scales; SA = Sieberg-Ambraseys (Ambraseys, 1962); SG = Soloviev and Go (Soloviev and Go, 1974). Catalogue code: 1 = Pasarić et al., 2012; 2 = NOAA/WDC Tsunami Event Database.

Map of the seismogenic sources in AD5. The CSS belonging to the AD5 are shown as labeled polygons with a red polyline. The ISS belonging to the AD5 are shown as labeled blue rectangles. For a general map of all Adriatic domain seismogenic sources see Figure 3.

The list of ISSs of AD5 with their parameters.

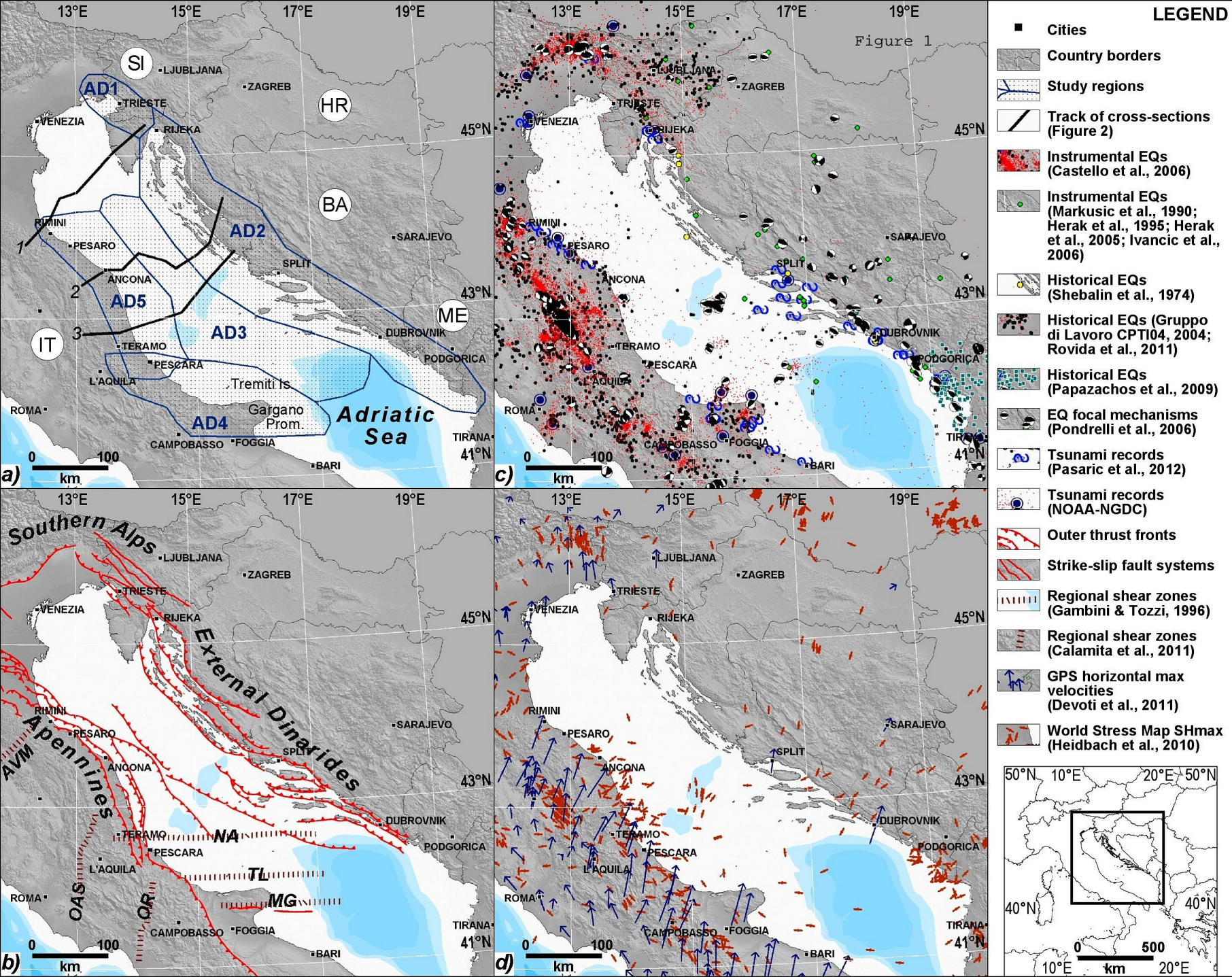
The list of CSSs of AD5 with their parameters.

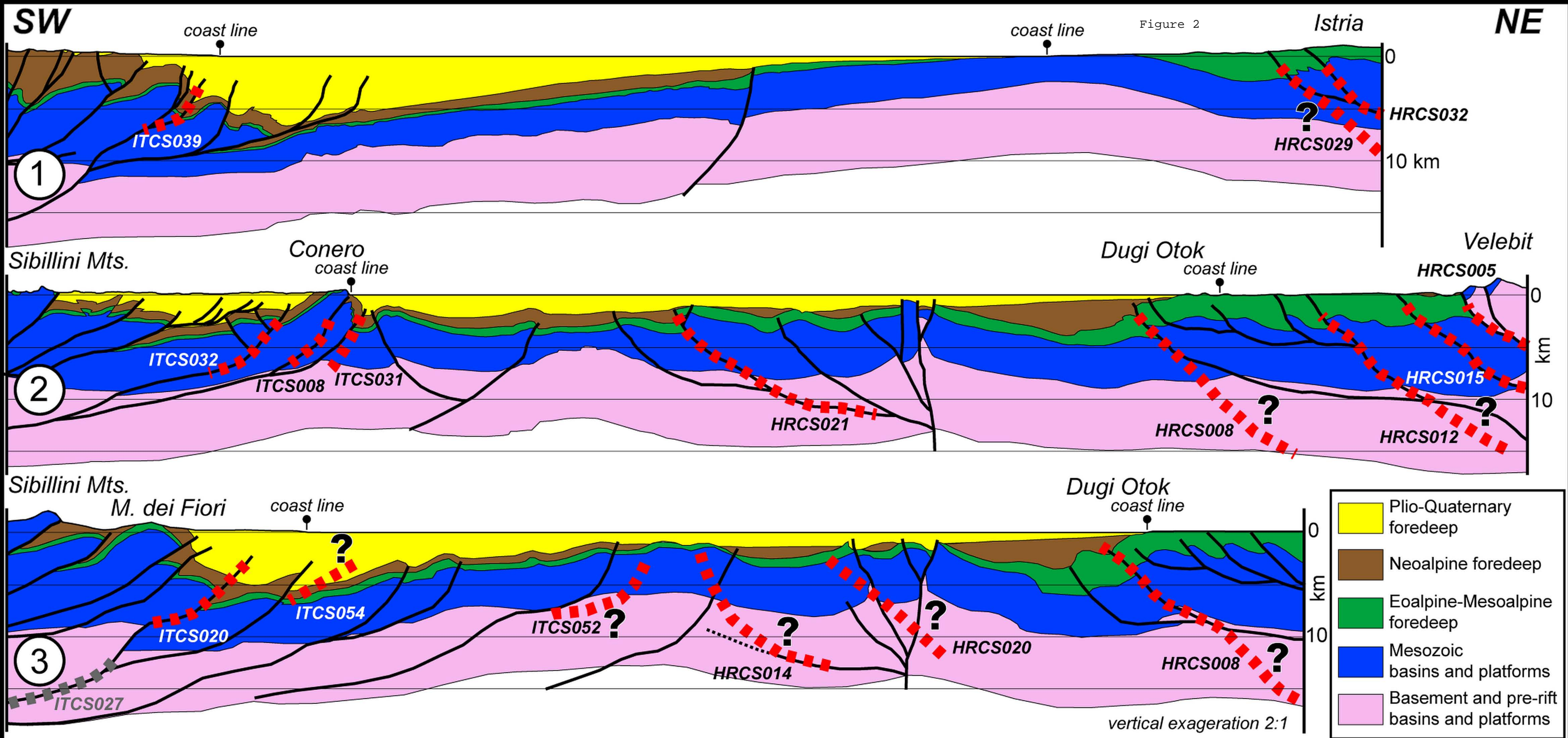
Figure 8:

Thematic maps of the Adriatic domain CSSs, showing their kinematic and activity parameters. The upper edge of the source is color-coded based upon the legend presented in each image slot. a) CSSs classified by their average faulting style; b) CSSs classified by their maximum magnitude values; c) CSSs classified by minimum slip rates; d) CSSs classified by maximum slip rates.

Figure 9:

Seismotectonic sketch of the active deformation in the Adriatic domain. 1: External Dinarides, SW verging active thrusting; 2: Apennines, NE verging active thrusting; 3: Southern Alps, S verging active thrusting; 4: dextral strike-slip domains; 5: average maximum horizontal stress axis.





Region name	North-Eastern Adriatic
Region code	AD1
Structural setting	External Dinarides thrust belt
Principal faulting style	reverse to reverse-dextral strike slip
Largest Earthquake	14.08.1574 M_w 5.6 Lupoglav earthquake
Largest Tsunami	26.03.1511 I 2 Venice/Trieste tsunami

ASSOCIATED EARTHQUAKES

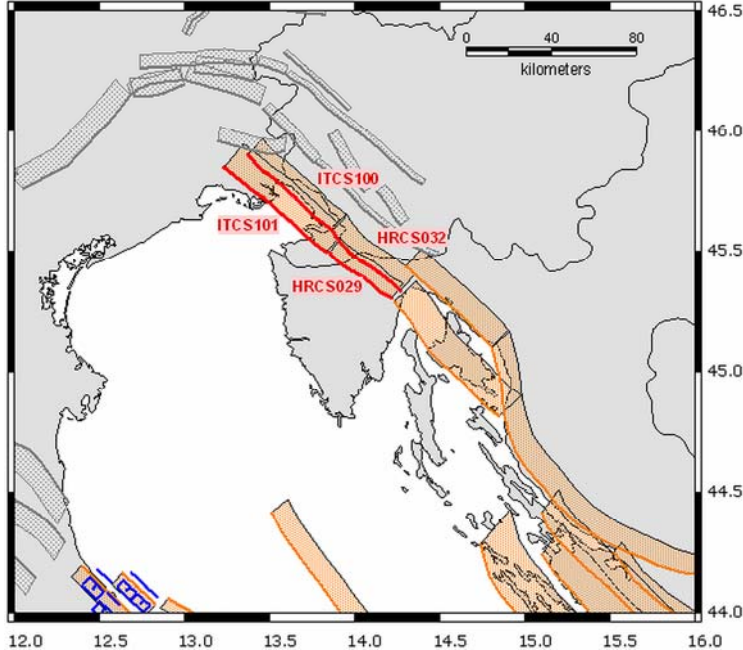
yyyy-mm-dd	Longitude	Latitude	Magnitude	Intensity	Catalogue code	Associated ISS	Associated CSS
1574-08-14	14.10	45.40	5.6	8	1	/	HRCs029

List of earthquakes $M \geq 5.5$ and/or $l \geq 8$ in the region. More details in captions.

ASSOCIATED TSUNAMIS

yyyy-mm-dd	Localities affected	Reliability	Intensity SA	Intensity SG	Catalogue code
1511-03-26	Venice/Trieste	definite	2	5	1

List of registered tsunamis in the region. More details in captions.



Graphical representation image of seismogenic sources of the region.

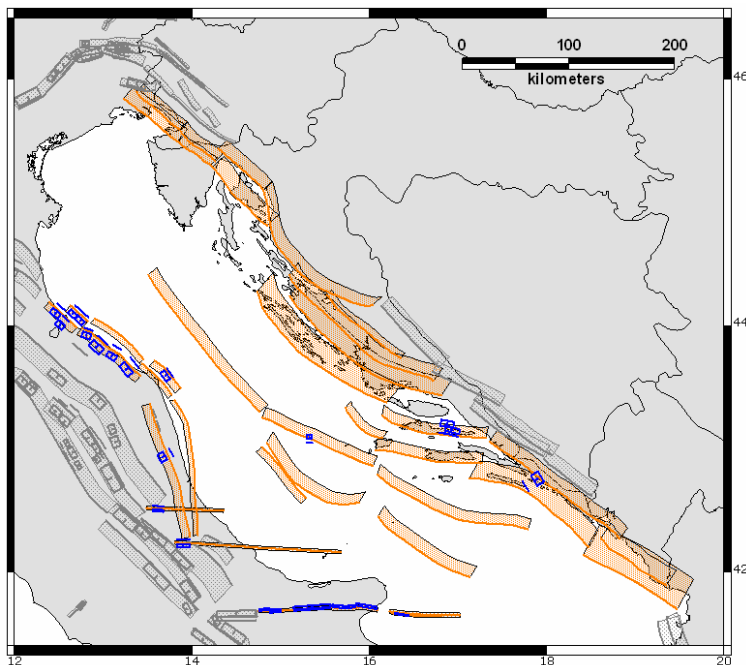


Image of seismogenic sources of the region (red polylines).

INDIVIDUAL SEISMOGENIC SOURCES

IDSource	SourceName	Length (km)	Width (km)	Depth (km)	Strike (deg)	Dip (deg)	Rake (deg)	Average displacement (m)	Reccurance Interval (yr)	Latest earthquake	Max Mag
no data for this area											

List of Individual Seismogenic Sources (ISS). Taken from DISS 3.2.0 available with a complete data set at <http://diss.rm.ingv.it/diss/>.

COMPOSITE SEISMOGENIC SOURCES

IDSource	SourceName	Depth (km)	Strike (deg)	Dip (deg)	Rake (deg)	Slip Rate (mm/yr)	Max Mag
HRCs029	Lupoglav	1 - 11	320 - 340	40 - 60	120 - 140	0.1 - 0.3	6.0
HRCs032	Trstenik	1 - 15	320 - 340	50 - 60	130 - 160	0.1 - 0.3	6.5
ITCS100	Northern Trieste Gulf	1 - 15	320 - 350	50 - 60	130 - 160	0.1 - 0.3	6.5
ITCS101	Southern Trieste Gulf	1.5 - 12	320 - 350	30 - 45	100 - 120	0.1 - 0.3	6.5

List of Composite Seismogenic Sources (CSS). Taken from DISS 3.2.0 available with a complete data set at <http://diss.rm.ingv.it/diss/>.

Region name	Eastern Adriatic
Region code	AD2
Structural setting	Internal and central part of External Dinarides thrust belt
Principal faulting style	thrusting, reverse to reverse-dextral strike slip
Largest Earthquake	06.04.1667 M_w 7.2 Dubrovnik earthquake
Largest Tsunami	06.04.1667 I 4 Dubrovnik tsunami

ASSOCIATED EARTHQUAKES

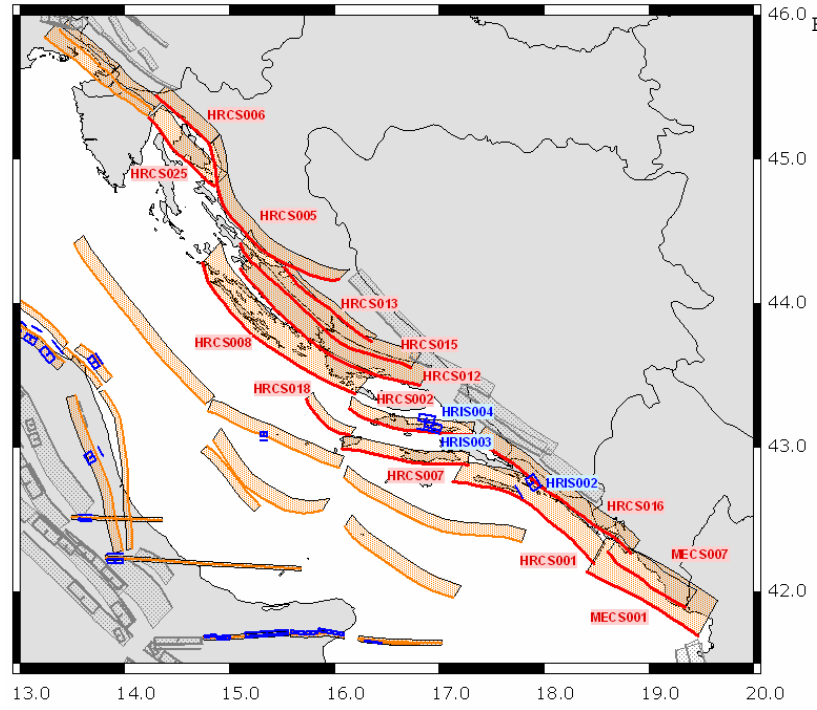
yyy-mm-dd	Longitude	Latitude	Magnitude	Intensity	Catalogue code	Associated ISS	Associated CSS
1323	14.70	45.20	6.0	9	1	/	HRCS005
1343-06-30	15.00	44.00	/	9	5	/	HRCS008
1563-06-13	18.50	42.40	7.0	/	8	/	HRCS001
1608-08-04	18.60	42.50	6.3	/	8	/	HRCS016
1639-07-28	18.30	42.50	6.8	/	8	/	HRCS001
1648	14.90	44.90	/	8	5	/	HRCS006
1667-04-06	18.10	42.60	7.2	10	5,8	/	HRCS001
1699	19.20	41.90	6.2	/	4	/	MECS001
1721-01-12	14.40	45.30	6.1	9	1	/	HRCS025
1844	16.70	43.50	/	8	5	/	HRCS012
1870-03-01	14.40	45.40	5.6	8	1	/	HRCS005
1878-09-23	14.90	45.00	/	8	5	/	HRCS006
1916-03-12	14.80	45.20	5.6	8	1	/	HRCS005
1956-08-15	15.95	43.21	5.8	/	3	/	HRCS018
1962-01-07	16.88	43.20	5.9	/	3	HRIS004	HRCS002
1962-01-11	16.94	43.15	6.1	/	3	HRIS003	HRCS002
1979-04-15	19.00	41.97	7.1	/	4	/	MECS001
1996-05-09	17.90	42.76	6.0	/	6	HRIS002	HRCS001

List of earthquakes M≥5.5 and/or I≥8 in the region. More details in captions.

ASSOCIATED TSUNAMIS

yyyy-mm-dd	Localities affected	Reliability	Intensity SA	Intensity SG	Catalogue code
1667-04-06	Dubrovnik	definite	/	4	1
1838-08-10	Rijeka	questionable	/	3	1
1844-03-22	Dubrovnik	questionable	/	2	2
1870-07-29	Vis	very improbable	2	/	1
1845-08-16	Gruž (Dubrovnik)	definite	/	3	1
1962-01-11	Split, Makarska, Brač	definite	2	3	1
1979-04-09	Montenegro	very doubtful	/	/	2
1979-04-15	Bar, Dubrovnik, Bar, Ulcinj	definite	4	1	1

Legend: List of registered tsunamis in the region. More details in captions.



Graphical representation of seismogenic sources of the region (red polylines).

INDIVIDUAL SEISMOGENIC SOURCES

IDSource	SourceName	Length (km)	Width (km)	Depth (km)	Strike (deg)	Dip (deg)	Rake (deg)	Average displacement (m)	Reccurance Interval (yr)	Latest earthquake	Max Mag
HRIS002	Ston-Slano	11	8.8	5.8 - 10.5	328	32	92	0.40	286 - 2000	1996-09-05	6.0
HRIS003	Hvar South	13	8.8	4-2 - 11.9	286	61	22	0.58	414 - 1933	1962-01-11	6.1
HRIS004	Hvar North	12	7.1	5.2 - 9.8	280	40	43	0.37	264 - 1233	1962-01-07	5.9

List of Individual Seismogenic Sources (ISS). Taken from DISS 3.2.0 available with a complete data set at <http://diss.rm.ingv.it/diss/>.

COMPOSITE SEISMOGENIC SOURCES

IDSource	SourceName	Depth (km)	Strike (deg)	Dip (deg)	Rake (deg)	Slip Rate (mm/yr)	Max Mag
HRCS001	Mljet	2 - 15	280 - 330	30 - 45	70 - 110	0.2 - 1.4	7.2
HRCS002	Hvar	2 - 15	260 - 310	40 - 70	20 - 70	0.3 - 1.4	6.5
HRCS005	Velebit	1 - 18	255 - 355	45 - 70	80 - 140	0.1 - 0.5	6.5
HRCS006	Vinodol - Rijeka	1 - 15	310 - 325	45 - 60	100 - 140	0.2 - 0.4	6.0
HRCS007	Vis-Korcula	2 - 15	270 - 290	40 - 70	20 - 70	0.1 - 0.6	5.8
HRCS008	Dugi Otok	2 - 18	280 - 330	30 - 45	90 - 120	0.1 - 0.5	6.0
HRCS012	Zadar	2 - 15	270 - 320	30 - 45	95 - 130	0.1 - 0.5	6.5
HRCS013	Novigrad	1 - 10	295 - 340	45 - 70	95 - 130	0.1 - 0.4	6.5
HRCS015	Benkovac	1 - 11	295 - 340	30 - 45	95 - 130	0.1 - 0.4	6.0
HRCS016	Peļjesac-Kotor	1 - 10	280 - 320	30 - 45	80 - 110	0.3 - 1.0	6.5
HRCS018	Vis-West	2 - 15	280 - 330	50 - 70	90 - 120	0.1 - 0.5	5.8
HRCS025	Krk	1 - 15	320 - 340	40 - 50	110 - 130	0.1 - 0.3	6.0
MECS001	Montenegro offshore	2 - 15	290 - 310	15 - 40	80 - 100	0.9 - 2.0	7.2
MECS007	Budva offshore	1 - 10	270 - 350	25 - 35	80 - 110	0.15 - 1.2	6.5

List of Composite Seismogenic Sources (CSS). Taken from DISS 3.2.0 available with a complete data set at <http://diss.rm.ingv.it/diss/>.

Region name	Central Adriatic
Region code	AD3
Structural setting	External parts of the External Dinarides and Apennines, Middle Adriatic
Principal faulting style	thrusting
Largest Earthquake	02.07.1844 M_w 5.6 Adriatic earthquake
Largest Tsunami	unknown

ASSOCIATED EARTHQUAKES

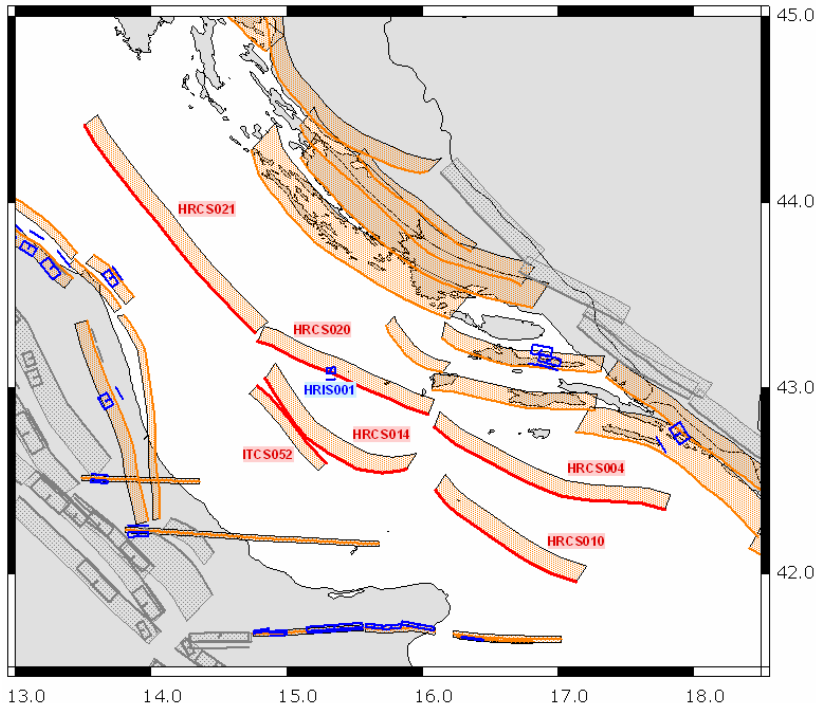
yyyy-mm-dd	Longitude	Latitude	Magnitude	Intensity	Catalogue code	Associated ISS	Associated CSS
1844-02-07	17.00	42.00	5.6	8	1	/	HRCS010
2003-03-29	15.30	43.10	5.5	/	7	HRIS001	HRCS020

List of earthquakes $M \geq 5.5$ and/or $I \geq 8$ in the region. More details in captions.

ASSOCIATED TSUNAMIS

yyyy-mm-dd	Localities affected	Reliability	Intensity SA	Intensity SG	Catalogue code
no data for this area					

List of registered tsunamis in the region. More details in captions.



Graphical representation of seismogenic sources of the region (red polylines).

INDIVIDUAL SEISMOGENIC SOURCES

IDSource	SourceName	Length (km)	Width (km)	Depth (km)	Strike (deg)	Dip (deg)	Rake (deg)	Average displacement (m)	Reccurance Interval (yr)	Latest earthquake	Max Mag
HRIS001	<i>Jabuka island</i>	11	8.8	3 - 6.3	269	42	70	0.24	1200-4800	2003-03-29	5.5

List of Individual Seismogenic Sources (ISS). Taken from DISS 3.2.0 available with a complete data set at <http://diss.rm.ingv.it/diss/>.

COMPOSITE SEISMOGENIC SOURCES

IDSource	SourceName	Depth (km)	Strike (deg)	Dip (deg)	Rake (deg)	Slip Rate (mm/yr)	Max Mag
HRCS004	<i>Eastern Adriatic offshore - South</i>	2 - 12	270 - 330	35 - 60	70 - 100	0.05 - 0.25	6.0
HRCS010	<i>Palagruza</i>	2 - 12	275 - 350	35 - 50	70 - 100	0.08 - 0.25	6.0
HRCS014	<i>Jana-1</i>	2 - 12	275 - 350	35 - 50	70 - 100	0.1 - 0.2	6.0
HRCS020	<i>Eastern Adriatic offshore - Central</i>	2 - 12	270 - 330	35 - 60	70 - 100	0.05 - 0.2	6.0
HRCS021	<i>Eastern Adriatic offshore - North</i>	2 - 12	270 - 330	35 - 60	70 - 100	0.05 - 0.15	6.0
ITCS052	<i>Western Mid-Adriatic offshore</i>	3 - 8	130 - 150	30 - 45	80 - 100	0.1 - 0.5	5.5

List of Composite Seismogenic Sources (CSS). Taken from DISS 3.2.0 available with a complete data set at <http://diss.rm.ingv.it/diss/>.

Region name	Southern Western Adriatic
Region code	AD4
Structural setting	Apulian foreland shear zone
Principal faulting style	dextral strike-slip
Largest Earthquake	30.07.1627 M_w 6.7 Gargano earthquake
Largest Tsunami	30.07.1627 I 5 Gargano tsunami

ASSOCIATED EARTHQUAKES

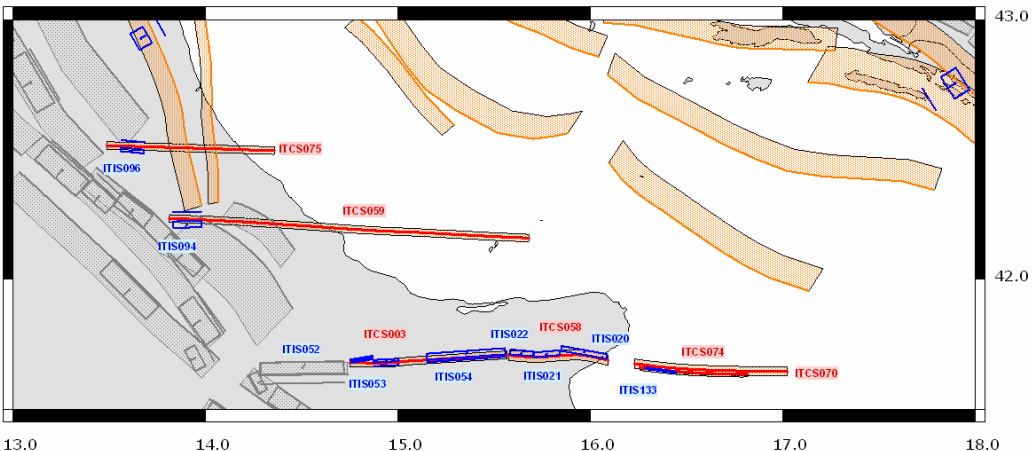
yyyy-mm-dd	Longitude	Latitude	Magnitude	Intensity	Catalogue code	Associated ISS	Associated CSS
1627-07-30	41.74	15.34	6.7	10	1	ITIS054	ITCS003
1646-05-31	41.73	15.76	6.6	9/10	1	/	ITCS058
1647-05-05	41.73	15.56	5.9	7/8	1	/	ITCS070
1657-01-29	41.73	15.39	6.4	8/9	1	/	ITCS003
1875-12-06	41.69	15.68	6.0	8	1	ITIS022	ITCS058
1948-08-18	41.58	15.75	5.6	7/8	1	/	ITCS058
1950-09-05	42.55	13.46	5.7	8	1	ITIS096	ITCS075
2002-10-31	41.70	14.93	5.7	7/8	1	ITIS052	ITCS003
2002-11-01	41.69	14.81	5.7	7	2	ITIS053	ITCS003

List of earthquakes M=>5.5 and/or Io=>8 in the region. More details in captions.

ASSOCIATED TSUNAMIS

yyyy-mm-dd	Localities affected	Reliability	Intensity SA	Intensity SG	Catalogue code
1627-07-30	<i>Lesina, Manfredonia</i>	definite	5	5	1,2
1731-03-20	<i>Siponto, Barletta</i>	definite	2	4	1,2
1889-12-08	<i>Termoli, Mattinata</i>	questionable	2	/	1

List of registered tsunamis in the region. More details in captions.



Graphical representation of seismogenic sources of the region (red polylines).

INDIVIDUAL SEISMOGENIC SOURCES

IDSource	SourceName	Length (km)	Width (km)	Depth (km)	Strike (deg)	Dip (deg)	Rake (deg)	Average displacement (m)	Recurrence Interval (yr)	Latest earthquake	Mag
ITIS096	<i>Isola del Gran Sasso</i>	10	6	12.0-17.8	95	75	225	0.25	500-2500	1950-09-05	5.7
ITIS094	<i>Tocco da Casauria</i>	12	8	11.0-18.5	89	70	230	0.45	900-4500	1456-12-30	6.0
ITIS053	<i>Ripabottoni</i>	9	8	12.0-20.0	261	86	195	0.18	360-1800	2002-11-01	5.7
ITIS052	<i>San Giuliano di Puglia</i>	11	8	12.0-19.9	267	82	203	0.20	400-2000	2002-10-31	5.8
ITIS054	<i>San Severo</i>	34	15	6.0-20.8	266	80	215	0.90	1800-9000	1627-07-30	6.7
ITIS022	<i>San Marco Lamis</i>	10	12	0.0-11.8	95	80	215	0.48	480-4800	1875-12-06	6.1
ITIS021	<i>San Giovanni Rotondo</i>	11	12	0.0-11.8	85	80	215	0.43	430-4300	/	6.1
ITIS020	<i>Monte Sant'Angelo</i>	20	12	0.0-11.8	280	80	215	0.67	558-1340	>1273 A.D.	6.4
ITIS133	<i>Gondola West</i>	13	7	0.5-7.5	278	85	225	0.30	405-1818	1893-08-10	6.0

List of Individual Seismogenic Sources (ISS). Taken from DISS 3.2.0 available with a complete data set at <http://diss.rm.ingv.it/diss/>.

COMPOSITE SEISMOGENIC SOURCES

IDSource	SourceName	Depth (km)	Strike (deg)	Dip (deg)	Rake (deg)	Slip Rate (mm/yr)	Max Mag
ITCS075	<i>Pietracamela-Montesilvano</i>	11.0-20.0	80-100	70-90	170-230	0.1-0.5	5.7
ITCS059	<i>Tocco Casauria-Tremiti</i>	11.0-20.0	80-100	70-90	170-230	0.1-1.0	6.0
ITCS003	<i>Ripabottoni-San Severo</i>	6.0-25.0	250-270	80-90	180-220	0.1-0.5	6.7
ITCS058	<i>San Marco in Lamis-Mattinata</i>	0.0-25.0	260-290	80-90	200-230	0.1-1.2	6.4
ITCS070	<i>Deep Gondola Fault Zone</i>	14.0-25.0	90-100	70-90	160-190	0.1-0.5	5.5
ITCS074	<i>Shallow Gondola Fault Zone</i>	0.0-14.0	270-280	80-90	220-230	0.1-1.0	6.5

List of Composite Seismogenic Sources (CSS). Taken from DISS 3.2.0 available with a complete data set at <http://diss.rm.ingv.it/diss/>.

Figure 6

Region name	Central Western Adriatic
Region code	AD5
Structural setting	External Apennines thrust belt
Principal faulting style	thrusting
Largest Earthquake	16.08.1916 M_w 6.1 Alto Adriatico earthquake
Largest Tsunami	30.10.1930 I 4 Senigallia tsunami

ASSOCIATED EARTHQUAKES

yyyy-mm-dd	Longitude	Latitude	Magnitude	Intensity	Catalogue code	Associate d ISS	Associate d CSS
1269-09	43.56	13.56	5.60	8	1	/	ITCS008
1672-04-14	43.94	12.58	5.60	8	1	/	ITCS039
1690-12-23	43.58	13.59	5.60	/	1	ITIS029	ITCS031
1786-12-25	43.99	12.57	5.60	8	1	ITIS035	ITCS039
1875-03-17	44.21	12.57	5.90	/	1	ITIS036	ITCS039
1897-09-21	43.71	12.97	5.50	7	1	/	ITCS032
1916-05-17	44.14	12.73	6.00	/	1	ITIS034	ITCS030
1916-08-16*	44.03	12.78	6.10	/	1	ITIS033	ITCS030
1916-08-16^	44.17	12.92	5.50	/	1	/	ITCS030
1930-10-30	43.66	13.33	5.80	8	1	ITIS030	ITCS032
1943-10-03	42.91	13.65	5.80	8/9	1	ITIS070	ITCS020

List of earthquakes M=>5.5 and/or I=>8 in the region. More details in captions.

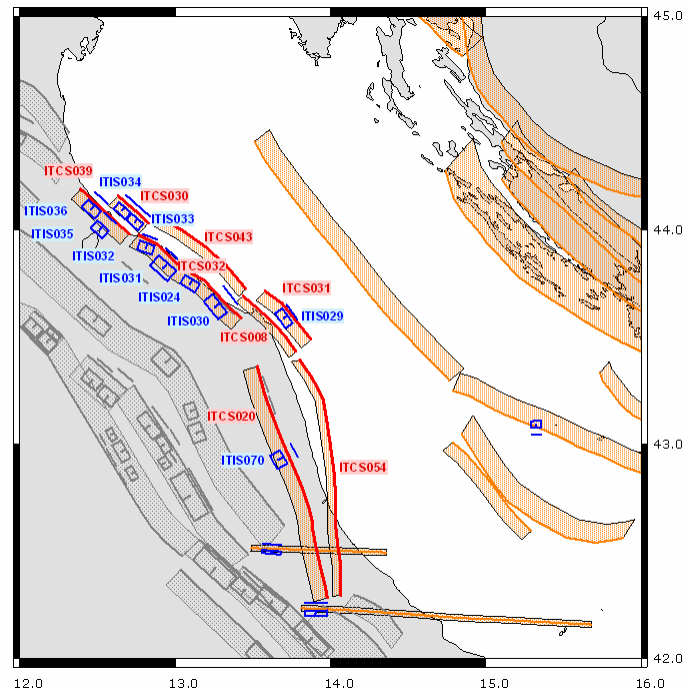
* = 07:06 (hh:mm)

^ = 08:15 (hh:mm)

ASSOCIATED TSUNAMIS

yyyy-mm-dd	Localities affected	Reliability	Intensity SA	Intensity SG	Catalogue code
1672-04-14	<i>Rimini</i>	definite	2	3	1,2
1875-03-17	<i>Cervia, Cesenatico, Pesaro</i>	definite	3	4	1,2
1916-08-16	<i>Tavollo</i>	definite	2	2	1,2
1930-10-30	<i>Ancona, Bakar</i>	definite	4	4	1,2

Legend: List of registered tsunamis in the region. More details in captions.



Graphical representation of seismogenic sources of the region (red polylines).

INDIVIDUAL SEISMOGENIC SOURCES

IDSource	SourceName	Length (km)	Width (km)	Depth (km)	Strike (deg)	Dip (deg)	Rake (deg)	Average displacement (m)	Reccurance Interval (yr)	Latest earthquake	Max Mag
ITIS036	<i>Val Marecchia</i>	9	6	3.0-6.0	132	30	90	0.27	540-2700	1875-03-17	5.7
ITIS035	<i>Rimini</i>	8	6	3.0-6.0	132	30	90	0.21	420-2100	1786-12-25	5.6
ITIS034	<i>Rimini offshore North</i>	8	5	3.0-5.5	132	30	90	0.36	720-3600	1916-05-17	5.7
ITIS033	<i>Rimini offshore South</i>	8	5	3.0-5.5	132	30	90	0.26	520-2600	1916-08-16	5.6
ITIS032	<i>Pesaro San Bartolo</i>	8	6	2.5-5.9	110	35	90	0.42	1167-1750	/	5.8
ITIS031	<i>Fano Ardizio</i>	12	8	3.0-7.0	132	30	90	0.60	1667-2500	/	6.1
ITIS024	<i>Mondolfo</i>	9	6	4.0-7.0	122	30	90	0.20	556-833	1924-01-02	5.6
ITIS030	<i>Senigallia</i>	12	7	4.0-7.5	142	30	90	0.40	1111-1667	1930-10-30	5.9
ITIS029	<i>Conero offshore</i>	9	6	2.5-6.4	145	40	90	0.40	800-4000	1690-12-23	5.9
ITIS070	<i>Offida</i>	8	7	4.5-8.7	150	35	90	0.40	800-4000	1943-10-03	5.9

List of Individual Seismogenic Sources (ISS). Taken from DISS 3.2.0 available with a complete data set at <http://diss.rm.ingv.it/diss/>.

COMPOSITE SEISMOGENIC SOURCES

IDSource	SourceName	Depth (km)	Strike (deg)	Dip (deg)	Rake (deg)	Slip Rate (mm/yr)	Max Mag
ITCS039	<i>Riminese onshore</i>	3.0-7.0	120-140	25-35	80-100	0.1-0.5	5.9
ITCS030	<i>Riminese offshore</i>	3.0-7.0	120-140	25-35	80-100	0.1-0.5	6.1
ITCS032	<i>Pesaro-Senigallia</i>	2.5-7.5	110-135	30-35	80-100	0.2-0.4	6.1
ITCS043	<i>Pesaro-Senigallia offshore</i>	2.5-6.5	110-145	30-45	80-100	0.1-0.5	5.5
ITCS008	<i>Conero onshore</i>	3.0-6.5	120-150	30-45	80-100	0.1-0.5	5.8
ITCS031	<i>Conero offshore</i>	2.0-7.0	120-150	30-45	80-100	0.1-0.5	5.9
ITCS020	<i>Southern Marche</i>	3.0-9.0	150-170	30-50	80-100	0.1-0.5	5.9
ITCS054	<i>Southern Marche offshore</i>	3.0-6.5	145-195	30-50	80-110	0.1-0.5	5.5

List of Composite Seismogenic Sources (CSS). Taken from DISS 3.2.0 available with a complete data set at <http://diss.rm.ingv.it/diss/>.

